UNCLASSIFIED

SECURITY CLASSIFICATION OF THIS PAGE (When Data Entered)

REPORT DOCUMENTATION PAGE		READ INSTRUCTIONS BEFORE COMPLETING FORM
1. REPORT NUMBER Final	2. GOVT ACCESSION NO.	3. RECIPIENT'S CATALOG NUMBER
4. TITLE (and Subtitle) The Cyclic Fatigue Behaviour of Adhesive Joints		5. TYPE OF REPORT & PERIOD COVERED Final (Dec 1992 to Dec 1995 6. PERFORMING ORG. REPORT NUMBER
7. AUTHOR(s) M. Fernando A.J. Kinloch		8. CONTRACT OR GRANT NUMBER(s) DAJA 45-93-C-0008 RSD 6869-MS-01
9. PERFORMING ORGANIZATION NAME AND ADDRESS Mechanical Engineering Dept, Imperial College, Exhibition Road, London, SW7 2BX, UK		10. PROGRAM ELEMENT, PROJECT, TASK AREA & WORK UNIT NUMBERS
11. CONTROLLING OFFICE NAME AND ADDRESS United States Army, European Research Office		12. REPORT DATE December 1995 13. NUMBER OF PAGES 51
14. MONITORING AGENCY NAME & ADDRESS(if different from Controlling Office) -		15. SECURITY CLASS. (of this report) Unclassified 15a. DECLASSIFICATION/DOWNGRADING SCHEDULE

16. DISTRIBUTION STATEMENT (of this Report)

-

DISTRIBUTION STATEMENT E
Approved for public release;
Distribution Unlimited

17. DISTRIBUTION STATEMENT (of the abstract entered in Block 20, if different from Report)

-

18. SUPPLEMENTARY NOTES

-

19960325 054

19. KEY WORDS (Continue on reverse side if necessary and identify by block number)
Adhesives, Aluminium Alloy, Bonding, Composites, Cyclic Testing, Durability, Fatigue, Fracture Mechanics, Modelling, Surface Pretreatments

20. ABSTRACT (Continue on reverse side if necessary and identify by block number)

The current programme has focussed on the adhesive bonding of fibre-composites, based upon thermoplastic polymeric matrices, and the adhesive bonding of aluminium alloys. In both cases a structural epoxy-film adhesive has been employed. The thermoplastic-composite substrates consisted of (i) carbon-fibre/PEEK and (ii) glass-fibre/PPS materials. For all the substrates a range of surface pretreatments has been studied. A fracture mechanics approach has been adopted, and both monotonically-loaded and cyclic-fatigue loaded tests have been undertaken. Also, tests have been conducted in both 'dry' and 'wet' environments. Finally, a model has been proposed which predicts the long-term fatigue failure of bonded lap joints from the short-term fracture mechanics data.

DD FORM 1 JAN 73 1473 EDITION OF 1 NOV 65 IS OBSOLETE

Unclassified

SECURITY CLASSIFICATION OF THIS PAGE (When Data Enter

AD NUMBER	DATE	DTIC ACCESSION NOTICE

1. REPORT IDENTIFYING INFORMATION

A. ORIGINATING AGENCY

Imperial College, London England, UK.

B. REPORT TITLE AND/OR NUMBER

The Cyclic Fatigue Behaviour of Adhesive Joints

C. MONITOR REPORT NUMBER

R&D 6896-MS-01

D. PREPARED UNDER CONTRACT NUMBER

DAJA45-93-C-0008

2. DISTRIBUTION STATEMENT

Approved for Public Release -
Distribution Unlimited.

(F)

REQUESTER:

1. Put your
on rever
2. Complet
3. Attach fc
mailed
4. Use unc
informa
5. Do not c
for 6 tc

DTIC:

1. Assign
2. Return

19960325 054

DTIC Form 50 OCT 95

PREVIOUS EDITIONS ARE OBSOLETE

DISCLAIMER NOTICE

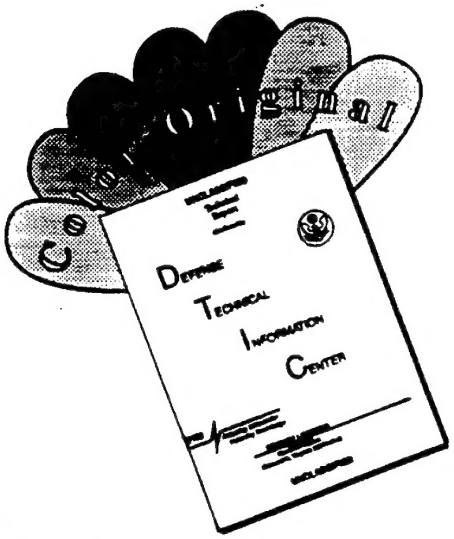

THIS DOCUMENT IS BEST QUALITY AVAILABLE. THE COPY FURNISHED TO DTIC CONTAINED A SIGNIFICANT NUMBER OF COLOR PAGES WHICH DO NOT REPRODUCE LEGIBLY ON BLACK AND WHITE MICROFICHE.

THE CYCLIC FATIGUE BEHAVIOUR OF ADHESIVE JOINT

by

M.FERNANDO and A.J.KINLOCH

CONTRACT NO:

DAJA 45-93-C-0008

DECEMBER 1995

INDEX

SECTION 1

INTRODUCTION

The current programme has focussed on the adhesive bonding of fibre-composites, based upon thermoplastic polymeric matrices, and the bonding of aluminium alloys. In both cases a structural epoxy-film adhesive has been employed.

Several main themes have been investigated:

(i) The effects of surface pretreatment of the composite or aluminium-alloy substrates prior to bonding.

(ii) The use of a fracture mechanics approach to measure the crack resistance of the bonded adhesive joints. Hence, to determine the value of the adhesive fracture energy, G_c.

(iii) An assessment of the lifetime of the adhesive joints when subjected to cyclic fatigue loading. Again, a fracture mechanics approach has been adopted to obtain the values of da/dN as a function of the maximum strain-energy release-rate, G_{max}, applied in the fatigue cycle. Of particular interest is whether a threshold value of the applied strain-energy release rate, G_{th}, below which no fatigue failure occurs, exists. Since, this has important implications for the design of adhesive joints. Obviously, if the applied loads on the joint are kept below a level corresponding to the value of G_{th}, then joint failure should not be observed, making due allowance of course for suitable safety factors.

(iv) The cyclic fatigue tests have also been conducted when the joints are immersed in water. Firstly, this is of interest because it represents a typical service-environment for adhesive joints. Secondly, because a major advantage of such 'wet' cyclic fatigue tests is that they may be undertaken and completed in the matter of a few weeks and do not require the use of unrealistically high temperatures or applied (static) loads in order to accelerate the mechanism of water attack upon the joints. Thus, the development and standardisation of 'wet' cyclic fatigue tests may provide the basis for a very effective accelerated-ageing test.

The following Sections of the report consider the fracture and fatigue of the fibre-composites bonded joints and of the aluminium-alloy bonded joints. The main conclusions are then discussed, and suggestions made for further work.

SECTION 2

ADHESIVELY-BONDED FIBRE-COMPOSITE JOINTS

2.1 Introduction

Polymer fibre-composites based upon thermoplastic matrices, such as poly(ether-ether ketone) and poly(phenylene sulphide), and containing carbon or glass fibres, offer significant advantages compared to those based upon thermosetting polymeric matrices such as epoxy resins. For example, thermoplastic fibre-composites may be readily thermoformed into components possessing a complex shape and usually exhibit a far higher interlaminar toughness [2.1]. However, in order to realise the full advantages from thermoplastic fibre-composites it is necessary to be able to join such composites to themselves, and to other materials, and to have confidence in the mechanical behaviour of the bonded joints.

One of the most widely employed methods for joining the more conventional thermosetting polymer fibre-composites is via the use of structural adhesives. This class of adhesives, typically based upon epoxy resins, possess a relatively high modulus and strength and are used to produce load-bearing joints. Now to obtain high strengths from joints which consist of thermosetting polymer fibre-composites bonded using structural adhesives is a relatively straightforward task [2.2]. Typically a simple abrasion treatment, followed by a solvent wipe to remove abraded debris, is sufficient to ensure that the locus of failure of the bonded joints is not at the adhesive/composite interface and that relatively tough and strong joints are formed.

However, Kinloch and Taig [2.3] observed that obtaining high strength joints when using the thermoplastic fibre-composites was far more difficult. They found that a simple abrasion and solvent-wipe treatment was an inadequate surface treatment prior to bonding for these materials, since this form of treatment led to the joints failing at the adhesive/composite substrate interface at a relatively very low failure load. Later work by Kinloch and co-workers [2.4-2.6] demonstrated that a surface treatment based upon exposing the thermoplastic-fibre composite to a "corona discharge" or an "oxygen-plasma" was, however, particularly effective. Joints employing such a surface treatment never failed at the adhesive/composite interface and possessed a high toughness and strength.

Further, it was found that the problem of poor adhesion of structural adhesives to thermoplastic-fibre composites appeared to be a general one; common, to a greater or lesser extent, to all such materials which were examined. It was found that after a certain, critical, intensity of corona or plasma treatment is employed for the thermoplastic fibre-composites the subsequently bonded joint no longer fails along the adhesive/composite interface. Instead, failure occurs either in the adhesive layer or in the fibre-composite substrate, and this change in the locus of failure is associated with a far higher value of the adhesive fracture energy, G_c.

The current work extends the previous studies, and examines the cyclic fatigue behaviour of bonded joints which consist of pretreated thermoplastic-based fibre-composites bonded using an epoxy-film adhesive.

2.2 Experimental

2.2.1 The materials

The adhesive employed was a hot-curing toughened-epoxy, in the form of a film supported on a non-woven carrier. The adhesive was 'AF-163-2M' (from 3M Co., USA), with nominal thickness of 240 μm.

The thermoplastic fibre-composites were:

(a) Unidirectional carbon-fibre/PEEK ("APC-2" composite from ICI plc) - a continuous carbon-fibre composite containing a volume fraction of fibres of about 60% and a matrix of thermoplastic poly(ether-ether ketone). The composite substrate was prepared by laying unidirectional tape into a twenty four-ply stack for the single lap joint (SLJ) and 48-ply stack for the double cantilever beam (DCB) joints, the ply direction being $[0^0]$. The sheets of material were prepared employing a heated press. The temperature of the press was 380^o C and a pressure of 1.4 MPa was applied for 5 minutes.

(b) Multidirectional S2 glass-fibre/PPS - a continuous glass-fibre composite in a matrix of thermoplastic poly(phenylene sulphide) manufactured by Quadrax Advanced Materials Systems Inc., USA. This was supplied already moulded in the form of sheets about 6 mm in thickness. The stacking sequence of the composite was $[(0^o/+45^o/90^o/-45^o)_4+45^o/-45^o]_S$.

2.2.2 Surface treatments

Several different surface treatments were examined:

(a) Abrasion/solvent-cleaning: this is the typical treatment used for preparing composites based upon thermosetting polymeric matrices and the composite sheets were lightly abraded using 180/220 mesh alumina, then wiped clean with methyl-ethyl ketone and allowed to dry.

(b) Corona discharge: this treatment involved exposing the thermoplastic composite sheets to an air plasma formed at atmospheric pressure. The major components of the corona discharge equipment were the generator producing high frequency (15-20 kHz) power (0.1-0.9 kW), the high-power transformer giving the high voltage (15-20 kV) and the high-power cables carrying the high-voltage to the electrodes and the treater-station. The equipment was designed to include two special features. Firstly, conventional corona can readily treat non-conducting materials but the transformer of the present equipment was redesigned to give good impedance and capacitance matching between the electrode and the composite. For conducting materials a modified electrode was

designed with a silicone rubber covering the surface whilst for non-conducting materials a conventional knife-edged electrode was used. The second feature was that the power output from the electrode was current controlled, and not voltage controlled. Hence the power output from the electrode was directly obtained from the power gauge of the generator. After a light abrasion and a solvent wipe treatment the thermoplastic-composite substrates were placed on an automatically controlled table which travelled horizontally backwards and forwards under the discharge electrode. The velocity of the table could be selected to be between 14.5 to 62 mm/s and the velocity was controlled accurately by a stepper motor and a pulse generator (0.1-4.8 kHz). The energy output per unit area from the electrode onto the composites may be determined from:

$$E = PN/LV \qquad (1.1)$$

where E is the energy output per unit area, P is the power of the high-frequency generator, N is the number of cycles of the table, L is the length of the treater and V is the velocity of the table.

(c) An R.F.-generated oxygen-plasma: the plasma unit employed was a "Plasmaprep 100 Plasma Chemistry unit" and its principal features were an aluminium barrel reactor chamber, which could be supplied with oxygen at a reduced pressure, and a radio-frequency (R.F.) power amplifier to generate the plasma. After a light abrasion and a solvent wipe treatment the thermoplastic-composite substrates were placed in the chamber and the air pressure reduced until it fell below about 200 mtorr, at which point oxygen was introduced into the chamber. The oxygen flow rate was regulated by a venturi meter and was adjusted to give a flow rate of 30 cm^3/min. When the oxygen pressure had dropped below 200 mtorr the RF power amplifier was switched on. The power was slowly increased and a forward power of 85 W was used, and the reflected power was noted to be 2.5 W.

In the present work, all the fibre-composite substrates were stored in a desiccator after surface treatment had been completed until they were bonded, as described below. The substrates were bonded within about 24 hours of treatment.

2.2.3 Joint preparation

Mode I (tensile-opening) double-cantilever beam (DCB) test specimens, schematically shown in Figure 2.1, were prepared. The width of the test specimen was 20 mm and the length was about 150 mm. The nominal thickness of the PEEK fibre-composites substrates was about 6 mm and of the PPS fibre-composites was also approximately 6 mm.

The DCB joints were prepared by placing a rectangular length of the film adhesive onto a strip of fibre-composite and then laying a release-coated aluminium foil, about 75 mm in length, between the adhesive film and the composite substrate, before bringing the adhesive film and the substrates into contact. (This resulted in an initial (interfacial) crack length of about 75 mm.) The adhesive was then cured by heating the joint to 95^{o}C (as measured by a

thermocouple placed in the adhesive layer) for 90 minutes and then raising the temperature to 120°C for 30 minutes. The heat was then switched off and the joints were allowed to cool in the oven overnight. Whilst curing the adhesive joints were kept under a relatively low applied load. The glass transition temperature of the cured adhesive was 108°C. When the joint was cool, aluminium-alloy loading-blocks were bonded at the end of the DCB joint where the release-coated aluminium-alloy foil had been placed. These were bonded onto the fibre-composite substrates using a cold-cured epoxy-paste adhesive ('Permabond E38' from Permabond, UK). To help monitor the position of the crack front, the side of the specimen was painted using typewriter correction fluid, and marked at 5 mm intervals. It was important to apply only a thin coating, so that the crack length recorded was the actual crack length in the specimen, and was not simply the cracking of the correction fluid either ahead or behind the actual crack tip.

Single-lap joints were also prepared using the carbon-fibre/PEEK and glass-fibre/PPS composite substrates. For these lap joints, the former composite was 3 mm in thickness and 25.4 mm in width and the overlap length was 12.7 mm. For the lap joints based upon the glass-fibre/PPS composite, the material was 6 mm in thickness and 25.4 mm in width and the overlap length was varied from 12.7 to 50.0 mm.

2.2.4 Determination of the adhesive fracture energy, G_c

Tests were conducted at a constant rate of displacement of the crosshead of the tensile testing machine in order to ascertain the value of the adhesive fracture energy, G_c, of the adhesive. The rate of displacement used for the DCB adhesive joint test specimens was 1.0 mm/min.

In the double-cantilever beam (DCB) adhesive joint test, as shown in Figure 2.1, the two composite arms of the specimen are subjected to equal and opposite bending moments. Linear elastic fracture mechanics (LEFM) is applicable to the bonded aluminium-alloy joints and the value of mode I adhesive fracture energy, G_c, may be calculated via the equation [2.7]:

$$G_c = \frac{P_c^2}{2b} \cdot \frac{dC}{da} \qquad (2.2)$$

where P_c is the fracture load, b is the width of the specimen, C is the compliance ($C = \delta/P$; where δ is the displacement) and a is the crack length.

The value of the adhesive fracture energy, G_c, may also be expressed from 'simple beam theory' by [2.8]:

$$G_c = \frac{12 P_c^2 a^2}{b^2 h^3 E_s} \qquad (2.3)$$

where b is the width and h is the thickness of a fibre-composite arm, a is the crack length, P_c is the critical load required to induce crack growth and E_s is the axial modulus of the fibre-composite arms.

However, the above equation needs to be corrected [2.9] for various effects which are not accounted for in the simple beam theory used above. Such effects arise due to (i) large deflections of the arm, (ii) stiffening of the arms due to the presence of the end blocks and (iii) shear deformation and deflection at the crack tip. The large deflection and end-block effects may be taken into account by using the correction factors F and N. The values of F and N may be found from the expressions previously given [2.9]:

$$F = 1 - \Theta_1(\delta / L)^2 - \Theta_2(\delta l_1 / L)^2 \qquad (2.4)$$

where l_1 is the distance of the load-point above the beam axis, L is the length of the arms of the specimen (i.e. L=a) and δ is the displacement of the arms of the DCB specimen, and:

$$N = 1 - \Theta_3(l_2 / L)^3 - \Theta_4(\delta l_1 / L^2) - \Theta_5(\delta / L)^2 \qquad (2.5)$$

where l_2 is the half-width of the end-block. For the mode I DCB specimen, the values of the constants are:

$$\Theta_1 = 3/10; \Theta_2 = 3/2; \Theta_3 = 1; \Theta_4 = \frac{9}{8}[1 - (l_2 / a)^2]; \Theta_5 = 9/35 \qquad (2.6)$$

The correction factor, χ_I, may be introduced [2.9] for end-rotation and deflection of the crack tip. The value of χ_I may be ascertained from the expression for the corrected compliance, C, where:

$$C = \frac{\delta}{P} = \frac{8N(a + \chi_I h)^3}{bh^3 E_s} \qquad (2.7)$$

Now, from Equation (2.7), the value of χ_I may be deduced by plotting $(C/N)^{1/3}$ versus the corresponding value of the crack length, a, and the intercept yields the value of the correction factor χ_I. Also, from the slope of the linear relationship the value of E_s may be determined.

A typical plot of $(C/N)^{1/3}$ versus the corresponding value of the crack length, a, is shown in Figure 2.2, and an excellent linear relationship is obtained. The average value of χ_I deduced for the DCB joints based upon glass-fibre/PPS substrates bonded using the epoxy-film adhesive was 1.04.

The expression for the modulus, E_s, of the fibre-composite arms which may be determined from the DCB joint tests is now given by:

$$E_s = \frac{P}{\delta}\frac{8N(a+\chi_I h)^3}{bh^3} \qquad (2.8)$$

The moduli for the glass-fibre PPS composite deduced from the above Equation was 41.1±2.6 GPa. In order to confirm these measurements a three-point bend test was conducted for this fibre-composite and these tests yielded a value of 38 GPa. (In the three point bend test moduli were obtained for various span lengths and a graph was constructed of the inverse of the modulus against the thickness/span length ratio. The reciprocal of the intercept of this graph yielded the true modulus quoted above.) The good agreement between the value of E_s deduced from the DCB test and the independent three-point bend test confirms that the above analyses are correct.

The corrected value of the adhesive fracture energy, G_c, may be deduced from either the 'corrected-load' method:

$$G_c = \frac{12FP_c^2(a+\chi_I h)^2}{b^2h^3E_s} \qquad (2.9)$$

or the 'corrected-displacement' method:

$$G_c = \frac{3}{2}\frac{F}{N}\frac{P_c\delta_c}{b(a+\chi_I h)} \qquad (2.10)$$

where δ_c is the critical displacement.

2.2.5 Fracture mechanics data from the fatigue tests

The DCB adhesive test specimen was used to obtain the values of da/dN as a function of G_{max} and a sine-wave loading-form was employed at a frequency of 5 Hz. The displacement ratio ($\delta_{ratio} = \delta_{min}/\delta_{max}$) was 0.5 and the mean displacement was 1.5 mm.

The maximum value of the strain-energy release-rate, G_{max}, applied during a fatigue cycle may be deduced using:

$$G_{max} = \frac{P_{max}^2}{2b}\frac{dC}{da} \qquad (2.11)$$

where P_{max} is the maximum load applied during the fatigue cycle.

It should be noted that G_{max} has been employed, as opposed to ΔG, since during the unloading part of the fatigue cycle the debonded surfaces typically come into contact, resulting in facial interference of the adhesive with itself (if cohesive-in-the-adhesive failure occurs) or with the substrate surface (if interfacial failure occurs). This leads to the generation of surface debris which prevents the crack from fully closing when it is unloaded, and hence may give an artificially high value of G_{min}. Thus, it has been suggested [2.10,2.11] that it is better to use G_{max}, instead of ΔG; and this convention has been followed in the present studies. However, the choice of this approach does not significantly effect the general form of the fatigue crack-growth relationships.

The crack length as a function of the number of cycles was determined either (i) by using a travelling microscope, with the side of the DCB specimen painted white in order that the crack could be seen more clearly, or (ii) by using an ultrasonic 'A' scan method. The values of the crack length determined from these two different methods were in excellent agreement. The method employed for obtaining values of the crack growth rate per cycle, da/dN, was that described as the "incremental polynomial method" in ASTM E647-88 [2.12]. Several methods were investigated [2.11] for deducing the value of da/dN associated with a given crack length from the experimental measurements of crack length, a, versus number of cycles, N. The "incremental polynomial method" was found to be the most accurate, and the one that gave the lowest scatter. The value of G_{max} was determined using Equation (2.11).

For the tests conducted in the 'dry' environment, the test temperature was $23\pm1^{o}C$ and the relative humidity was 55%. For the tests conducted in the 'wet' environment, the test temperature was $26\pm2^{o}C$ and the joints were immersed in distilled water for about five minutes before the fatigue tests were started.

2.2.6 Single-lap joint tests

The single-lap joints were subjected to a constant rate of displacement tests and were tested at a rate of 0.5 mm/min. They were also subjected to cyclic fatigue tests and a sine-wave loading-form at a frequency of 5 Hz was employed. The load ratio was 0.5. The test temperature was $23\pm1^{o}C$ and the relative humidity was 55%. The number, N_f, of cycles needed for the lap joint to fracture was measured as a function of the maximum applied load per unit width, T_{max}, imposed on the lap joints in each cycle.

2.3. Results and Discussion

2.3.1 The bonded carbon-fibre/PEEK joints

2.3.1.1 The values of G_c

Firstly, it was found that a simple abrasion/solvent wipe pretreatment gave very, very low joint strengths, with failure occurring at the adhesive/composite interface. These observations are in agreement with previous work [2.3,2.4]. Therefore, an additional corona or plasma treatment stage is needed for the thermoplastic composite prior to bonding. The level of corona treatment needed to obtain cohesive failure through the adhesive for the carbon-fibre/PEEK was about 30 J/mm^2. Both corona and plasma treatments of the carbon-fibre/PEEK composite prior to bonding were found to be adequate to avoid interfacial failure, and the associated weak joints.

Secondly, for the carbon-fibre/PEEK joints which were so-treated, the value of the adhesive fracture energy, G_c, under monotonic loading was determined from Equation (2.2) to be 1300 J/m^2. The locus of joint failure was via a cohesive failure through the adhesive layer.

2.3.1.2 The cyclic fatigue behaviour

As was observed for the constant rate of displacement tests, for the corona treated carbon-fibre/PEEK substrates bonded using the epoxy film-adhesive, during the fatigue tests the crack propagated cohesively through the adhesive layer in a stable manner.

A typical graph of da/dN versus G_{max}, where the value of G_{max} was determined using Equation (2.11), is shown in Figure 2.3; using logarithmic scales. Several noteworthy points may be observed from these data. Firstly, the agreement between the duplicate tests for the fatigue experiments conducted in the 'dry' environment of 23±1°C and 55% r.h. is very good. Secondly, there is no significant effect of undertaking the fatigue tests in the 'wet' environment, where the test temperature was 26±2°C and the joints were immersed in distilled water for about five minutes before the fatigue tests were started. Thirdly, the data is described by a power-law relationship, as discussed below.

2.3.1.3 Single lap joint data

The carbon-fibre/PEEK substrates were again subjected to a level of corona treatment of about 30 J/mm^2 prior to being bonded. This gave a cohesive failure through the adhesive with a static lap joint strength of 41 MPa.

The fatigue results are shown in Figure 2.4 in the form of the maximum applied load per unit width, T_{max}, versus the number, N_f, of cycles needed for the lap joint to fail. Again, the locus of joint failure was cohesive failure through the adhesive layer.

2.3.1.4 Predictions of the fatigue life of lap joints

Predictive Model

A major aim of previous work has been to use the fracture mechanics data generated from the fatigue tests to predict the fatigue lifetime of adhesive joints of a design commonly used in industrial applications. Such a design of adhesive joint is the single-overlap joint loaded in tension, as used to generate the data shown in Figure 2.4.

Obviously, to employ the fracture mechanics data generated from the above studies, the strain-energy release-rate in a single lap-joint during cyclic fatigue loading needs to be deduced. This relationship may then be substituted into an expression which models the fracture mechanics data shown in Figure 2.3. This can then be integrated to give the number of cycles to failure, N_f, as a function of the load or stress applied during the fatigue cycle.

The analysis to perform these tasks is described below, and follows that discussed in detail in references [2.12,2.14,2.15].

Firstly, an expression which describes the complete relationship between logarithmic G_{max} versus logarithmic da/dN is given by:

$$\frac{da}{dN} = DG_{max}^{n}\left\{\frac{1-\left(\frac{G_{th}}{G_{max}}\right)^{n_1}}{1-\left(\frac{G_{max}}{G_c}\right)^{n_2}}\right\} \qquad (2.12)$$

where G_{th} is the minimum, or threshold, value of the applied strain-energy release-rate below which no fatigue crack growth is observed to occur, G_c is the value of the adhesive fracture energy from the constant rate of displacement tests and D, n, n_1 and n_2 are material constants.

Secondly, considering the value of G_{max} for the lap joint, then it is well documented that single-overlap joints loaded in tension fail due to the transverse (out-of-plane) tensile, or cleavage, stresses, σ_{11}, which act at right angles to the direction of the applied load. These stresses are mainly introduced by the eccentricity of the loading path. Now, the maximum value of the transverse tensile stress, σ_{11}, in a lap joint is given by:

$$\sigma_{11} = M_e\left(\frac{E_a}{2t_a X}\right)^{1/2} \tag{2.13}$$

where E_a and t_a are the modulus and thickness of the adhesive layer respectively. The bending stiffness, X, and the bending moment, M_e, per unit width are given by:

$$X = \frac{E_s h^3}{12(1-\upsilon^2)} \tag{2.14}$$

and:

$$M_e = 0.5KT(h + t_a) \tag{2.15}$$

where the bending moment factor, K, is given by:

$$K = \frac{1}{1+\varepsilon c} \tag{2.16}$$

where:

$$\varepsilon = \left(\frac{T}{X}\right)^{1/2} \tag{2.17}$$

and where E_s, h and υ are the modulus, thickness and Poisson's ratio of the substrate material, c is one half of the bonded overlap length and T is the load per unit width applied to the lap joint.

Now a very powerful method for deducing the strain-energy release-rate acting in a cracked beam is based upon a knowledge of the bending moments at the crack tip. For symmetrical loading, the mode I strain-energy release-rate, G, is given by:

$$G = \frac{12M_e^2}{E_s h^3} \tag{2.18}$$

Combining Equations (2.13-2.17), then the value of G_{max} may be expressed by:

$$G_{max} = \frac{12}{E_s h^3}\left(\frac{T_{max}(h+t_a)}{2}\right)^2\left(\frac{1}{(1+\varepsilon c)^2}\right) \qquad (2.19)$$

where T_{max} is the maximum applied load per unit width during a fatigue cycle.

The number of cycles to failure, N_f, of the single lap joint subjected to cyclic loading may be estimated by combining Equations (2.12) and (2.19), to eliminate G_{max}, and then by integrating between the limits of the initial flaw size, a_o, and the crack length, a_f, at which rapid fracture of the joint occurs. This gives:

$$N_f = \int_{a_o}^{a_f} \frac{DG_c^{n_2}[E_s h^3(1+\varepsilon[c-a])^2]^{n-n_2}}{[3(T_{max}\{h+t_a\})^2]^{n-n_1}} \cdot \frac{[G_c E_s h^3(1+\varepsilon[c-a])^2 - (3(T_{max}\{h+t_a\})^2]^{n_2}}{[3(T_{max}\{h+t_a\})^2 - G_{th}E_s h^3(1+\varepsilon[c-a])^2]^{n_1}} . da \qquad (2.20)$$

In this equation the values of the fracture mechanics parameters (i.e. D, n, n_1, n_2, G_{th} and G_c) may be deduced from the fatigue data obtained from the fracture mechanics specimens. Further, the geometry of the single-lap joint, whose fatigue behaviour is to be predicted is known; so the values of the parameters ε, h, t_a and c are known, as is the modulus, E_s, of the substrate materials forming the lap joint. So, if the values of the integration limits can be identified, then the number of cycles to failure, N_f, of the single lap joint may be predicted as a function of the maximum load per unit width, T_{max}, of the joint applied during a fatigue cycle. The integration limits, a_0 and a_f, represent the initial (Griffith) flaw size and the length of the fatigue crack when fast fracture occurs respectively, and may be readily calculated.

Comparison of theory and experiment

The theoretical predictions from Equation 2.20 for the fatigue lifetimes of the single lap joints are compared to the experimental data in Figure 2.5. The various parameters used in the analyses are given in Table 2.1, and these parameters are directly determined from the present experimental results. It should be noted that the Griffith flaw size, of 705 μm, for this joint system is somewhat larger than the values we have previously observed for other adhesive/substrate combinations. This may be due to an inherent manufacturing defect in the 'as-manufactured' joints, and evidence for initial defects of this size was seen from the ultrasonic C-scans conducted on the single lap joints prior to fatigue testing.

Table 2.1

Parameters used to calculate theoretically the fatigue lifetimes of the single lap joints using the fracture mechanics data.

Fracture energy of the adhesive	Gc (J/m^2)	1300
Strain energy release rate at threshold	Gth (J/m^2)	225
Modified Paris law coefficient of the adhesive	D(m^2/N.cycle)	3.82×10^{-20}
Modified Paris law exponent of the adhesive	n	4.3
Curve fitting constant for the adhesive(threshold region)	n_1	5
Curve fitting constant for the adhesive(fast fracture region)	n_2	60
Modulus of the substrate	E_s (GPa)	134
Modulus of the adhesive	E_a (GPa)	2.4
Fracture stress of the adhesive	σ_a (MPa)	38
Adhesive bondline thickness	t_a (mm)	0.2
Half the overlap length	c (mm)	6.35×10^{-3}
Poisson's ratio of the adhesive	υ	0.29
Thickness of the composite substrate	h (mm)	3.0
Griffith flaw size	a_o (μm)	705

As may be seen from Figure 2.5, the agreement between the experimental and theoretical predictions is excellent, confirming the validity of this approach as a useful means of predicting the fatigue failure in single lap joints, based upon a knowledge of a number of parameters extracted from the fracture mechanics tests. Clearly, the approach enables long-term fatigue lifetimes to be predicted using the results from relatively short-term fracture mechanics experiments.

Now, the physical mechanism which the model is based upon is one of fatigue crack growth through the adhesive joint, whilst the joint is subjected to the cyclic loading. To study whether this actually occurred we have taken ultrasonic C-scans of the single lap joints.

Figure 2.6 shows a colour C-scan of the different stages of crack growth in a fatigue experiment. The first scan shows an 'as-made' joint which is essentially free of large defects, while the second scan depicts the extent of crack growth in the same joint after 1.5 million cycles of fatigue loading. As assumed in the crack growth model, crack propagation does indeed originate from the edges of the single lap joint, and propagates towards the centre. The third scan shows the amount of crack growth after 2 million cycles, and the fatigue crack is clearly propagating in towards the centre of the joint from both edges, as assumed in the theoretical model.

2.3.2 The bonded glass-fibre/PPS joints

2.3.2.1 The values of G_c

The first set of tests used a simple abrasion and solvent wipe treatment for the glass-fibre/PPS substrates prior to bonding. The DCB joints were then prepared and tested and it was found that all the joints failed by interlaminar failure of the fibre-composite. Obviously, this was somewhat surprising, since it was thought from both the previous and the current work that some form of corona or plasma treatment for the fibre-composite substrates would have been necessary in order to prevent interfacial failure occurring at the composite/adhesive interface.

The reasons for the observation that just a simple abrasion/solvent wipe treatment appears to be adequate to avoid interfacial failure are considered to be:

(i) The presence, and exposure by the surface treatment of the glass fibres - glass has a high surface energy and is therefore a relatively easy material to bond.

(ii) The low transverse strength of the glass-fibre/PPS composite, compared to the high transverse tensile-stresses generated around the inserted interfacial crack. (Indeed, the transverse strength of the glass-fibre/PPS composite was measured and found to be about 8.6±0.2 MPa, which is extremely low.)

(iii) The above factors lead to the fact that interlaminar failure is seen at a relatively low load, before interfacial failure can occur.

The values of the adhesive fracture energy, G_c, were determined from using Equations (2.2), (2.9) and (2.10). The results from these different methods of analysing the experimental measurements were in good agreement and the value of G_c as a function of the length of the propagating crack, a, is shown in Figure 2.7. As may seen a rising 'R-curve' exists, with the value of G_c, increasing as the crack propagates through the composite. This is undoubtedly due to the degree of fibre-bridging increasing as the interlaminar failure of the composite substrate propagates. However, there is considerable scatter in the data. This is considered to be due to the high tendency of the glass-fibre PPS composite to undergo interlaminar failure, and to the significant degree of fibre-bridging which was then observed. The value of the adhesive fracture energy, G_c, for the onset of crack growth is about 600±100 J/m^2. This is far lower than the value of 1300 J/m^2 recorded for the carbon-fibre/PEEK joints, when the locus of failure was cohesive in the adhesive.

Thus, the results from the work on bonding the glass-fibre/PPS composites are rather inconclusive, since we observed interlaminar failure of the composite substrate. This was considered to be due to the relatively low transverse strength of the composite, which led to a new crack initiating in the composite, in the region of the inserted interfacial crack. This new crack in the composite then grew in an interlaminar manner through the composite to give failure of the joint.

2.3.2.2 Single lap joint data

To try and study the above effects in a practical design of joint, the glass-fibre/PPS composite was bonded to form a single overlap joint. Again, a simple abrasion and solvent wipe treatment was used for the glass-fibre/PPS substrates prior to bonding. The lap joints were then prepared and a series of joints were made with a varying adhesively-bonded overlap length. They were tested at a constant rate of displacement and it was found that all the joints failed by interlaminar failure of the fibre-composite.

The results are shown in Figure 2.8, where the failure load per unit width is plotted against the length of the bonded overlap. The data shows the expected relationship between these two parameters [2.16]. The The reason for this observation of the interlaminar locus of joint failure is considered to be: (i) the presence, and exposure by the surface treatment of the glass fibres - glass has a high surface energy and is therefore a relatively easy material to bond; (ii) the low transverse strength of the glass-fibre/PPS composite, compared to the high out-of-plane tensile-stresses induced by the bending moments generated in a single overlap-joint loaded in tension, as discussed above; and (iii) hence the above factors lead to the fact that interlaminar failure is seen at a relatively low load, before interfacial failure can occur.

2.4 Conclusions

2.4.1 The bonded carbon-fibre/PEEK joints

For the carbon-fibre/PEEK joints it was found that a simple abrasion/solvent wipe pretreatment gave very, very low joint strengths, with failure occurring at the adhesive/composite interface. Therefore, an additional corona or plasma treatment stage is needed for the thermoplastic composite prior to bonding. The level of corona treatment needed to obtain cohesive failure through the adhesive for the carbon-fibre/PEEK was about 30 J/mm^2. Both corona and plasma treatments of the carbon-fibre/PEEK composite prior to bonding were found to be adequate to avoid interfacial failure, and the associated weak joints. For the carbon-fibre/PEEK joints which were so-treated, the value of the adhesive fracture energy, G_c, was determined from Equation (2.2) to be 1300 J/m^2. The locus of joint failure was via a cohesive failure through the adhesive layer.

As was observed for the constant rate of displacement tests, for the corona treated carbon-fibre/PEEK substrates bonded using the epoxy film-adhesive, during the fatigue tests the crack propagated cohesively through the adhesive layer in a stable manner. A typical graph of logarithmic da/dN versus logarithmic G_{max}, where the value of G_{max} is the maximum strain-energy release rate applied in a cycle, showed that the agreement between the duplicate tests for the fatigue experiments conducted in the 'dry' environment of 23±1^{o}C and 55% r.h. was very good. Also, there was no significant effect of undertaking the fatigue tests in the 'wet' environment, where the test temperature was 26±2^{o}C and the

joints were immersed in distilled water for about five minutes before the fatigue tests were started. It was also found that the fatigue data may be described by a power-law relationship.

For the studies on the single-overlap joints loaded in tension, the carbon-fibre/PEEK substrates were again subjected to a level of corona treatment of about 30 J/mm^2 prior to being bonded. This gave a cohesive failure through the adhesive with a static lap joint strength of 41 MPa. The fatigue behaviour of the lap joints was also measured. The relationship between the maximum load per unit width, T_{max}, and the number of cycles to failure, N_f, could be predicted extremely well from the fracture mechanics data.

2.4.2 The bonded glass-fibre/PPS joints

For the glass-fibre/PPS substrates bonded also using the epoxy-film adhesive, the first set of tests used a simple abrasion and solvent wipe treatment for the prior to bonding. The DCB joints were then prepared and tested and it was found that all the joints failed by interlaminar failure of the fibre-composite. Now it was thought that some form of corona or plasma treatment for the fibre-composite substrates would have been necessary in order to prevent interfacial failure occurring at the composite/adhesive interface. Clearly this was not the case. The reasons for the observation that just a simple abrasion/solvent wipe treatment appears to be adequate to avoid interfacial failure were considered to be:

(i) The presence, and exposure by the surface treatment of the glass fibres - glass has a high surface energy and is therefore a relatively easy material to bond.

(ii) The low transverse strength of the glass-fibre/PPS composite, compared to the high transverse tensile-stresses generated around the inserted interfacial crack. (Indeed, the transverse strength of the glass-fibre/PPS composite was measured and found to be about 8.6±0.2 MPa, which is extremely low.)

(iii) The above factors lead to the fact that interlaminar failure is seen at a relatively low load, before interfacial failure can occur.

However, the above factors are reflected in the fact that the value of the adhesive fracture energy, G_c, for the onset of crack growth is about 600±100 J/m^2. This is far lower than the value of 1300 J/m^2 recorded for the carbon-fibre/PEEK joints when the locus of failure was cohesive in the adhesive.

To try and study the above effects in a practical design of joint, the glass-fibre/PPS composite was bonded to form a single overlap joint. Again, a simple abrasion and solvent wipe treatment was used for the glass-fibre/PPS substrates prior to bonding. The lap joints were then prepared and a series of joints were made with a varying adhesively-bonded overlap length. They were tested at a constant rate of displacement and it was found that all the joints failed by interlaminar failure of the fibre-composite, even when a relatively long overlap length was employed.

2.5 References

2.1. F.N. Cogswell, 'Thermoplastic Aromatic Polymer Composites' (Butterworth, London, 1992)

2.2. A.J. Kinloch, 'Adhesion and Adhesives: Science and Technology' (Chapman and Hall, London, 1983) p 123

2.3. A.J. Kinloch and C.M. Taig, 'The Adhesive Bonding of Thermoplastic Composites' J. Adhesion **21** (1987) p 291

2.4. A.J. Kinloch and G.K.A. Kodokian, 'The Design of Double-Overlap Joints Using Thermoplastic Composites' J. Adhesion **37** (1992) p 33

2.5. A.J. Kinloch, G.K.A. Kodokian and J.F. Watts, 'The Adhesion of Thermoplastic Composites' Phil. Trans. Royal Soc. London **A338** (1992) p 83

2.6. B.R.K. Blackman, A.J. Kinloch and J.F. Watts, 'The Plasma Treatment of Thermoplastic Composites for Adhesive Bonding' Composites **25** (1994) p 332

2.7. A.J. Kinloch, 'Adhesion and Adhesives: Science and Technology' (Chapman and Hall, London, 1983) p 264

2.8. B.R.K. Blackman, J.P. Dear, A.J. Kinloch and S.O. Osiyemi, 'The Calculation of Adhesive Fracture Energies from DCB Test Specimens' J. Materials Sci. Letters **10** (1991) p 253

2.9. S. Hashemi, A.J. Kinloch and J.G. Williams, 'The Analysis of Interlaminar Fracture in Uniaxial Fibre-Polymer Composites' Proc. Royal Soc. London **A427** (1990) p 173

2.10. R.H. Martin and G.B. Murri, 'Characterisation of mode I and mode II delamination growth and thresholds in AS4/PEEK composites' ASTM STP **1059** (1990) p 251

2.11. S.O. Osiyemi, 'The fatigue performance of adhesively bonded fibre-composite joints', (Ph.D Thesis, Univ. of London, 1992), p 83

2.12. A.J. Kinloch and S.O. Osiyemi, 'Predicting the fatigue life of adhesively-bonded joints' J. Adhesion **43** (1993) p 79

2.13. ASTM, 'Standard test method for measurement of fatigue crack growth rates' E647 (1988)

2.14. J.K. Jethwa, 'The fatigue performance of adhesively-bonded metal joints', (Ph.D Thesis, Univ. of London, 1995)

2.15. J.K. Jethwa and A.J. Kinloch, 'The fatigue performance of adhesively-bonded metal joints', Proc. 17th Annual Meeting of the US Adhesion Soc., Florida, USA, February, 1994

2.16. A.J. Kinloch, 'Adhesion and Adhesives: Science and Technology' (Chapman and Hall, London, 1983) p 227

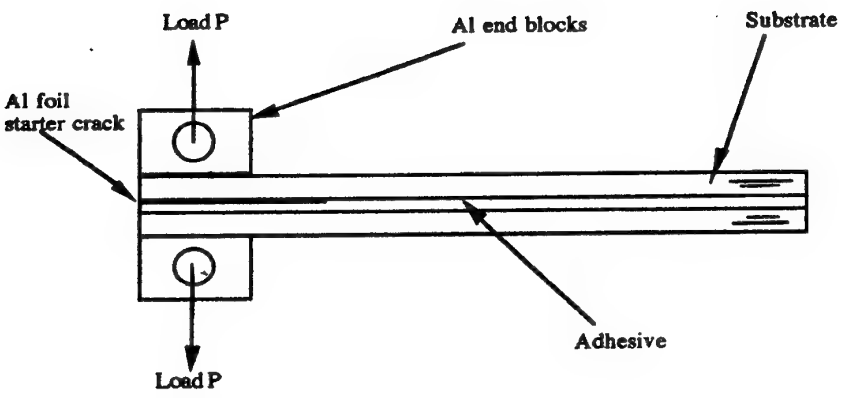

Figure 2.1 A schematic representation of the DCB joint.

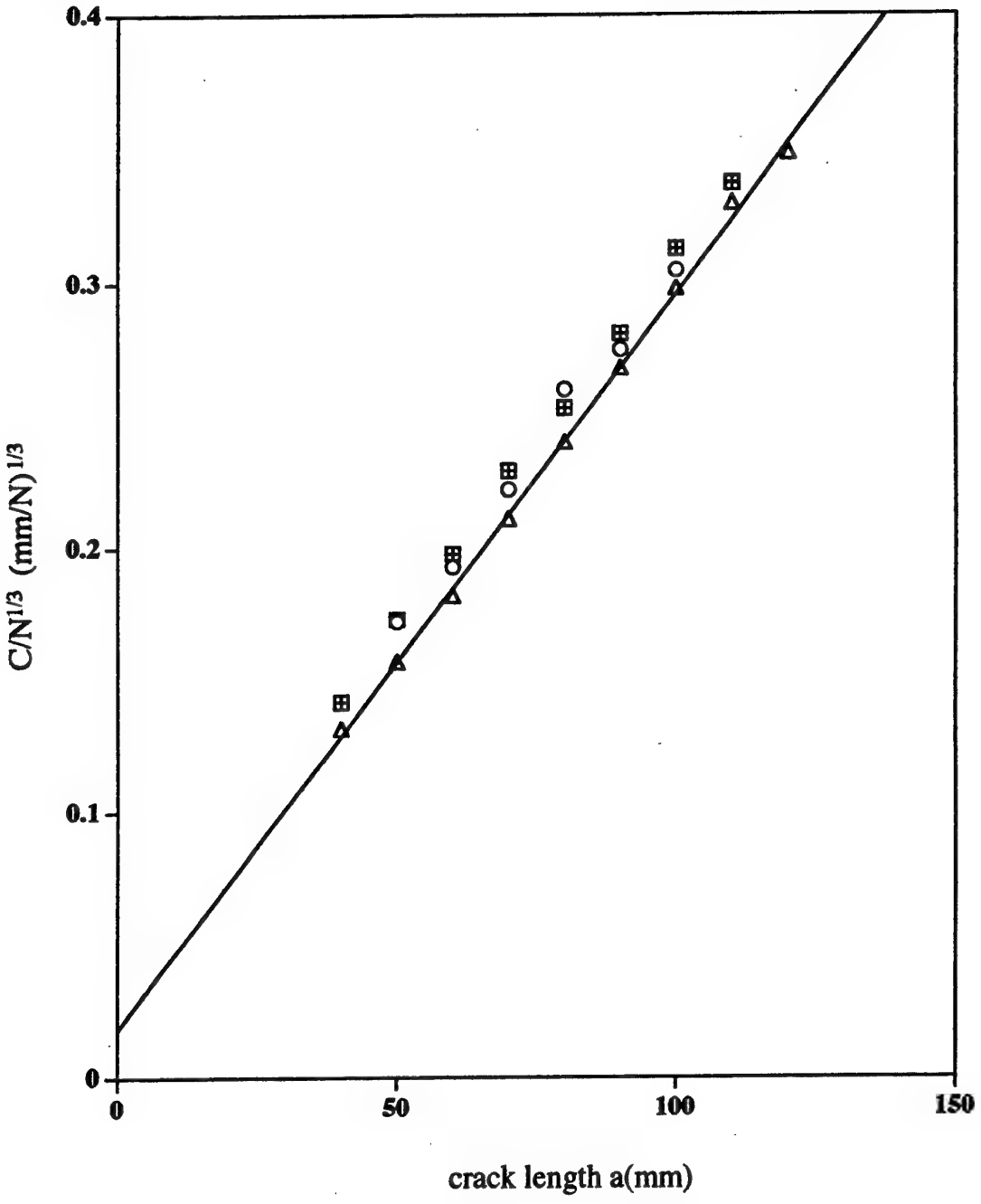

Figure 2.2 $(C/N)^{1/3}$ versus crack length, a for a DCB adhesive joint consisting of glass-fibre/PPS substrates bonded using the epoxy-film adhesive.

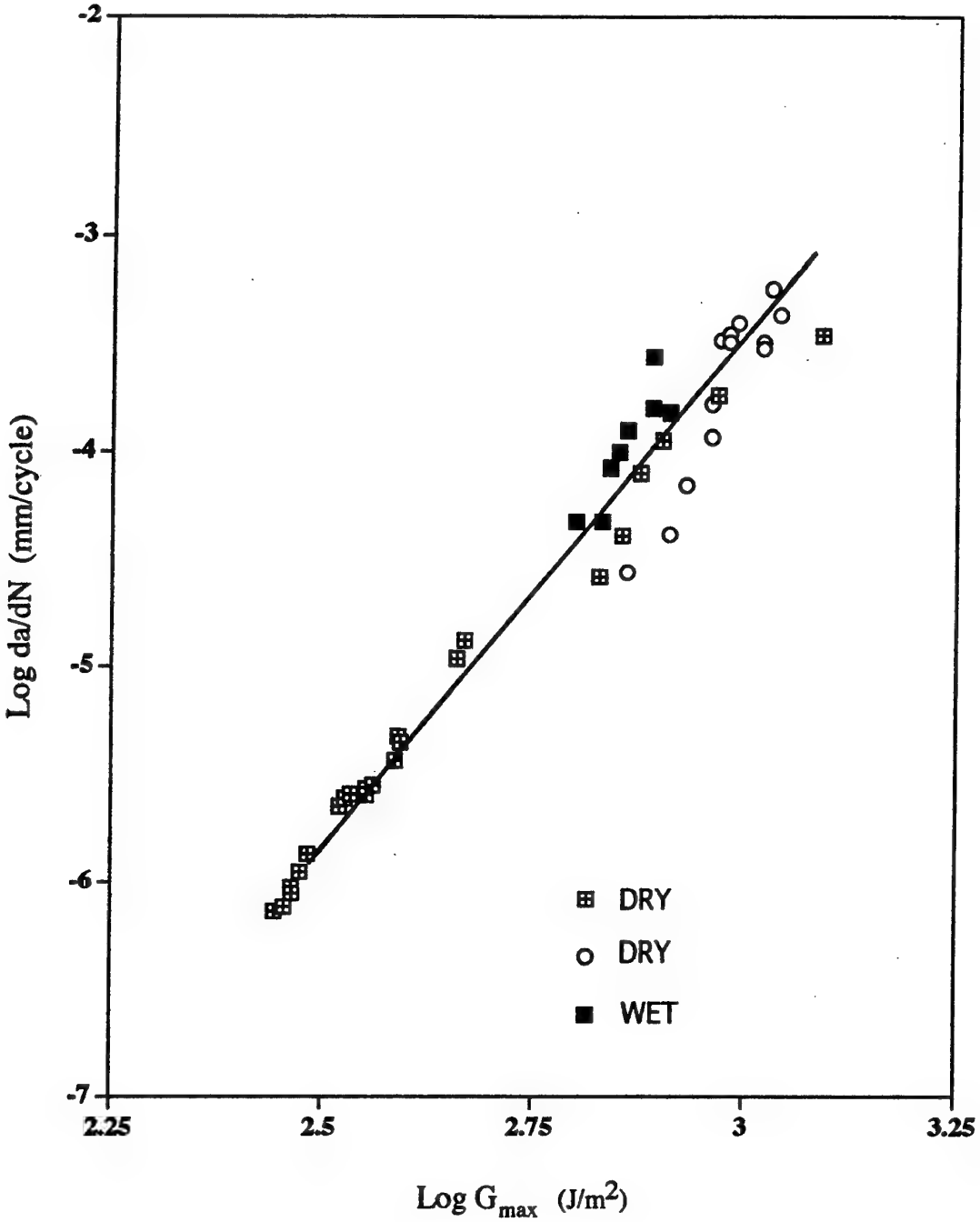

Figure 2.3 Log crack growth rate per cycle, da/dN, versus log G_{max} for the joints prepared using carbon-fibre/ PEEK substrates (corona treated)bonded with the epoxy film adhesive in the 'dry' and 'wet' environments.(DCB joints)

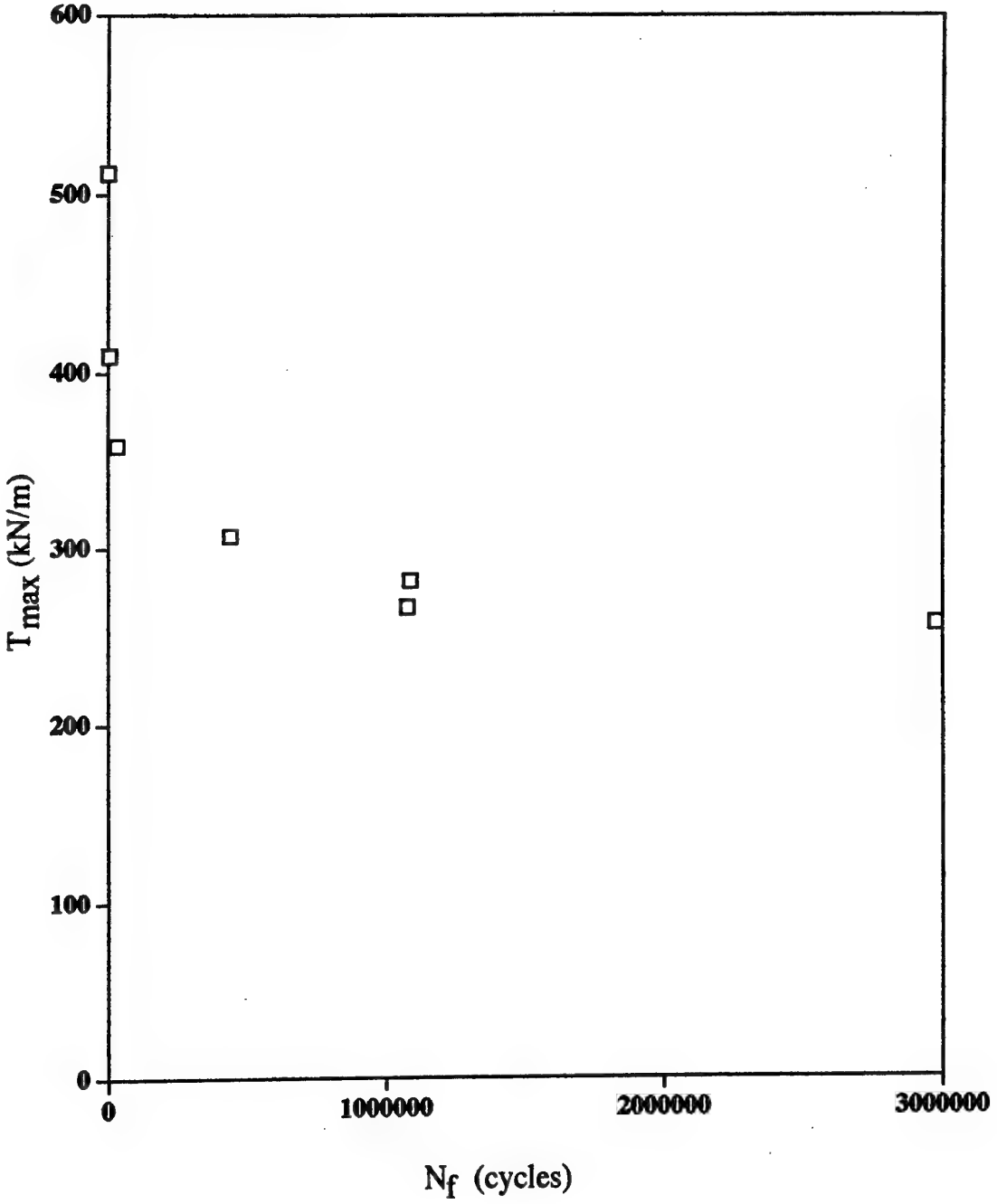

Figure 2.4 Experimental values for the maximum load per unit width, T_{max} applied in a fatigue cycle versus the number, N_f, of cycles to failure for the carbon-fibre/PEEK substrates(corona treated) bonded using the epoxy- film adhesive.(SLJ tests)

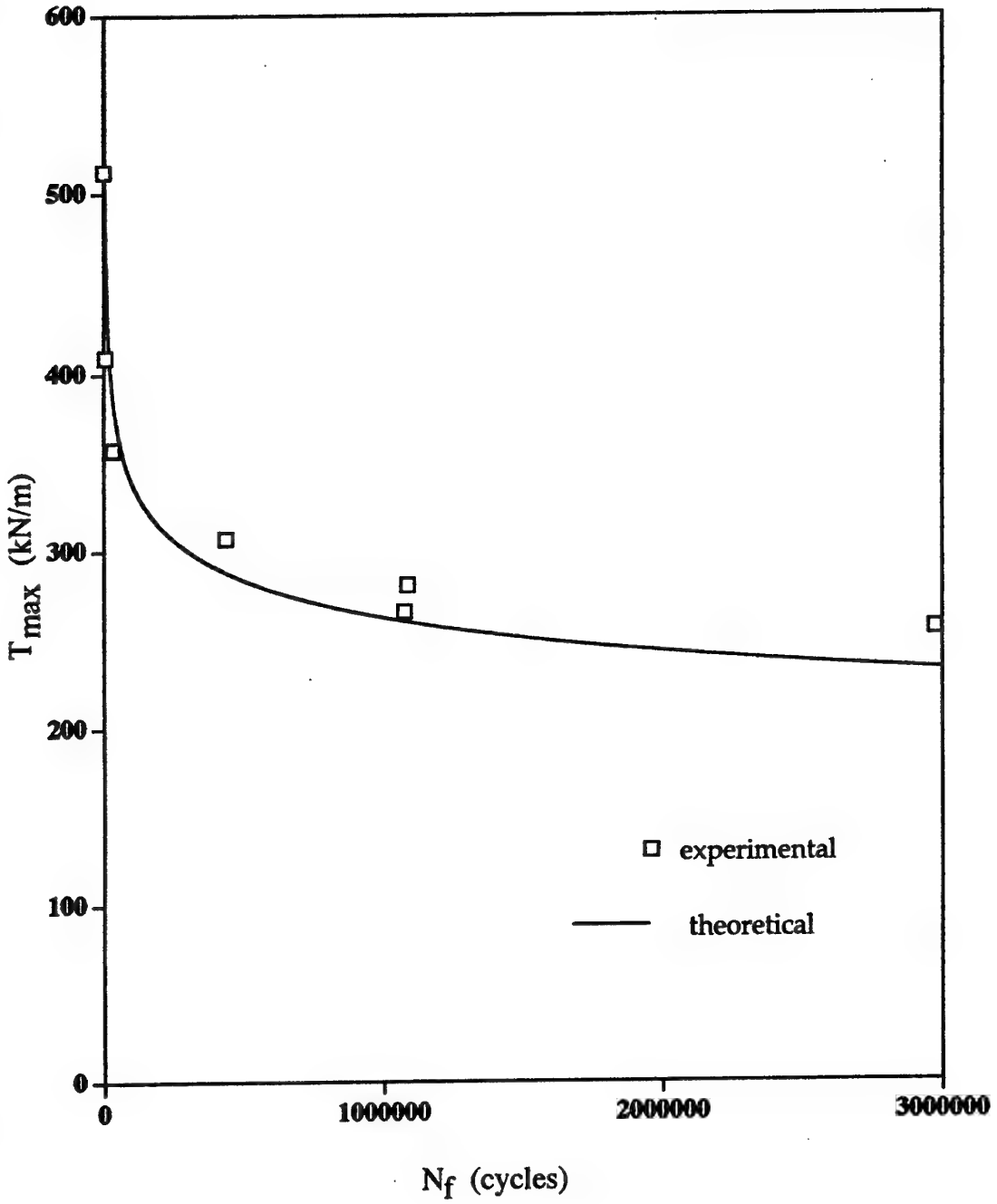

Figure 2.5 A comparison of the theoretical and experimental values for the maximum load per unit width, T_{max} applied in a fatigue cycle versus the number, N_f, of cycles to failure for the carbon-fibre/PEEK substrates(corona treated) bonded using the epoxy film adhesive. (Single lap joints)

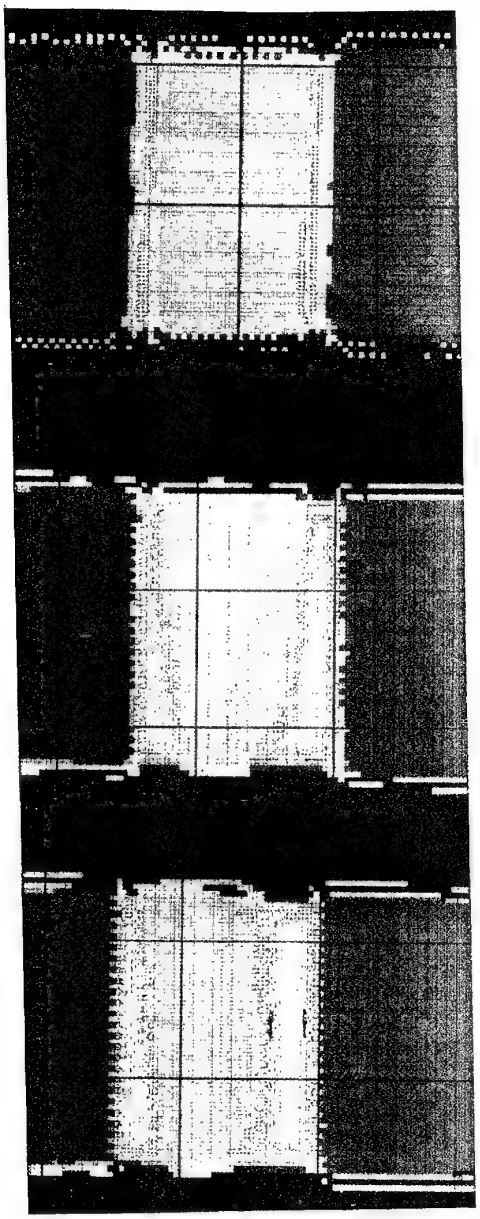

Figure 2.6 Ultrasonic C-scans of the carbon-fibre/PEEK single lap joints bonded using the epoxy-film adhesive. The upper scan is for an 'as-made' joint. The middle scan is for the same joint after 1.5 million fatigue cycles and the lower scan is for the same joint after 2.0 million fatigue cycles.

(The dark blue represents the carbon-fibre/PEEK substrates; the red is the bonded overlap of the joint; the light blue represents debonded regions steadily progressing through the joint from the edges towards the centre of the 'once-bonded' overlap.)

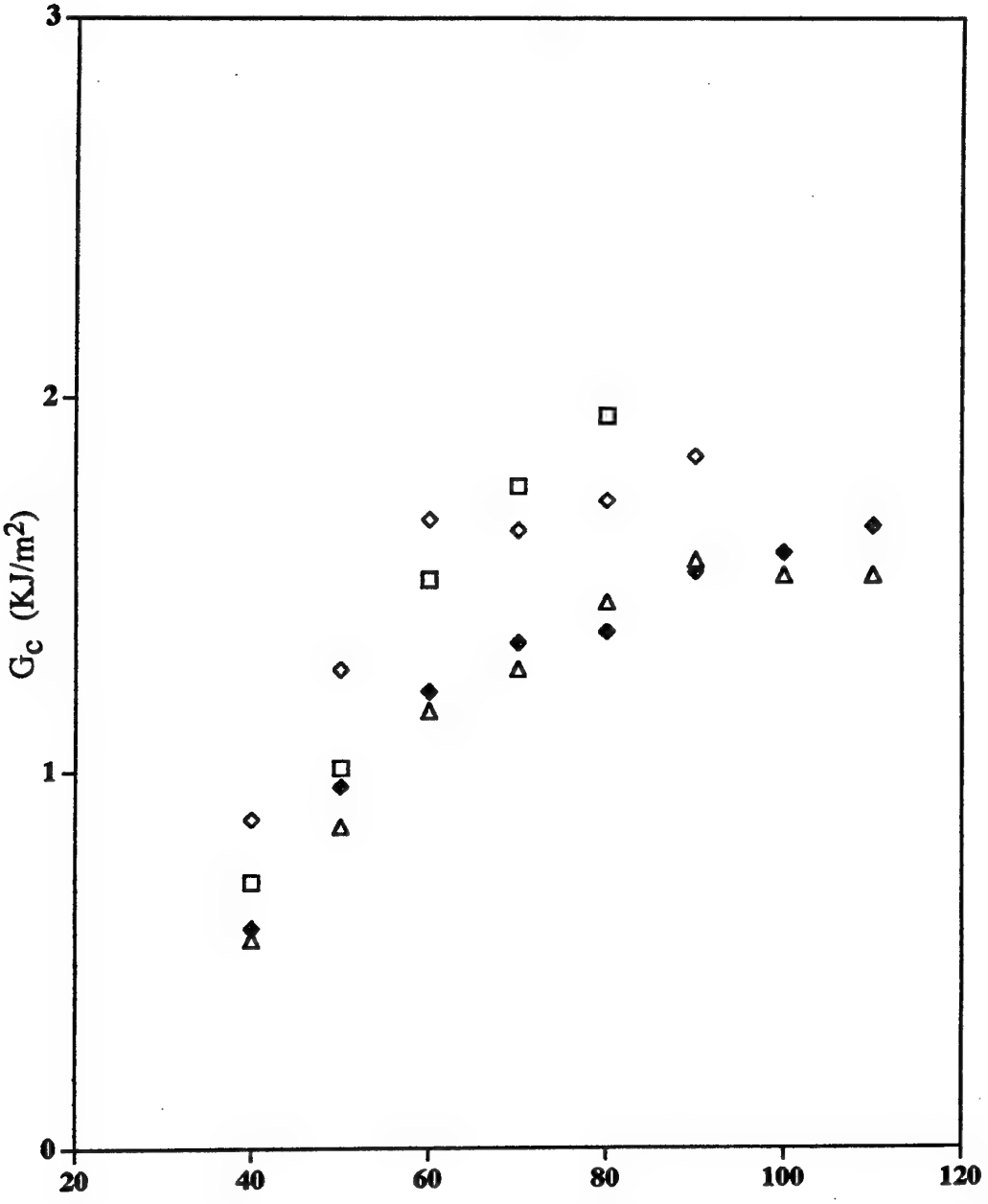

Figure 2.7 The adhesive fracture energy, G_c, versus the length, a, of the propagating crack for the joints consisting of the glass-fibre/PPS substrates(abrasion/solvent wipe treated) bonded using the epoxy film adhesive.(DCB tests.)

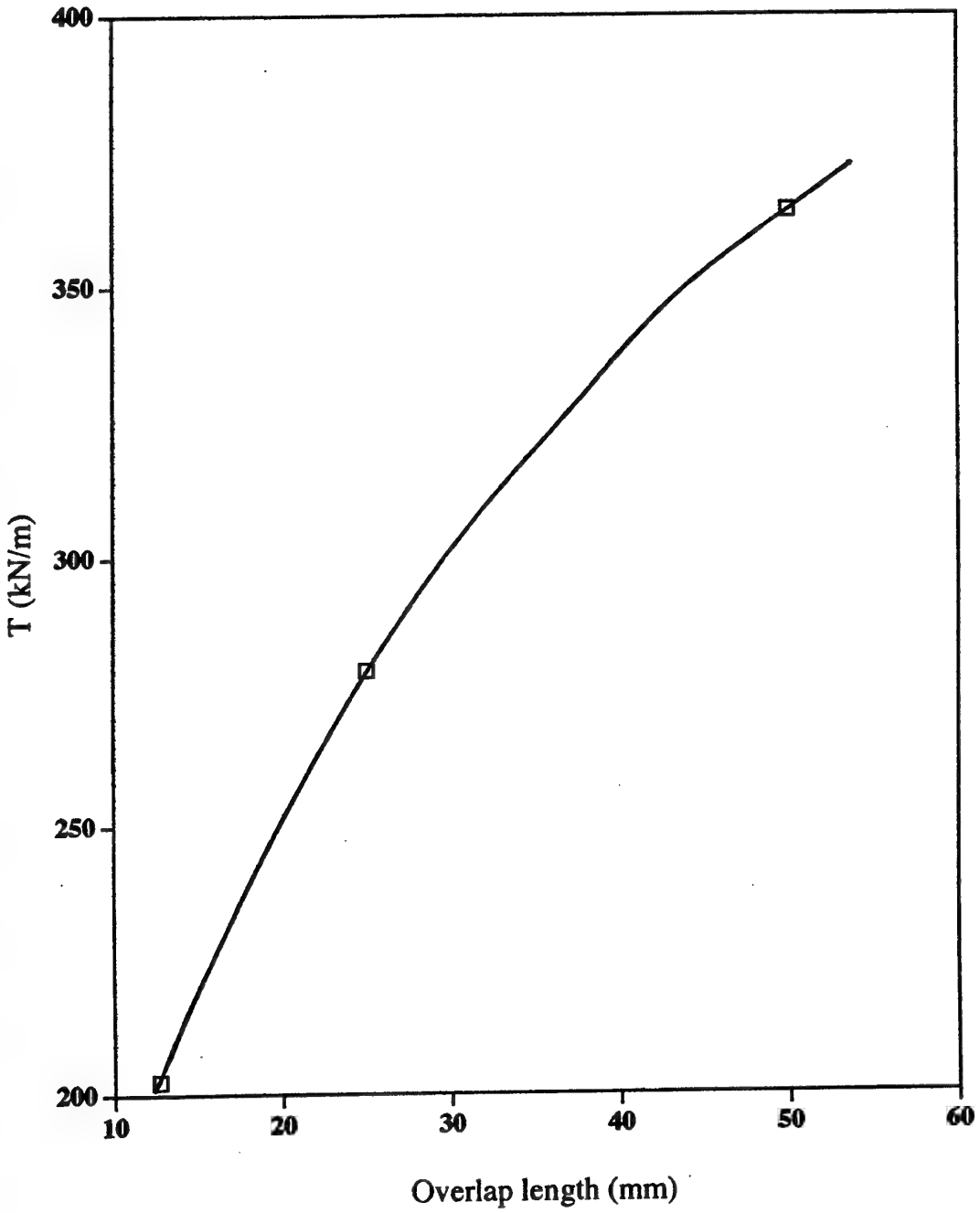

Figure 2.8 The failure load per unit width, T, versus the bonded overlap length for the joints consisting of the glass-fibre/PPS substrates (abrasion/solvent wipe treated) bonded using the epoxy-film adhesive. (Single lap joint tests.)

SECTION 3

ADHESIVELY-BONDED ALUMINIUM-ALLOY JOINTS

3.1. Introduction

Adhesive joints are frequently expected to perform satisfactorily under service conditions which include dynamically applied loads and exposure to hostile environments such as water, organic solvents, etc.; and, in many instances, combinations of these conditions may be experienced. It is therefore of prime importance for the adhesives technologist to be able to develop and recommend adhesive systems which will possess an adequate service life under the operating conditions which are to be experienced by the bonded structure. This, in turn, leads to the need to understand the mechanisms of failure and to develop test methods for (i) developing and selecting adhesive systems and (ii) predicting, quantitatively, the expected service life.

Dynamic fatigue is the phenomenon of failure or fracture of a material, joint or structure under repeated or oscillatory loading [3.1]. The importance of dynamic fatigue is that under fluctuating loads joints will fail at stress levels much lower than they can withstand under monotonic loading or under static (i.e. creep) loading. Further, it is well established that the mechanical performance of adhesive joints may be adversely affected when exposed to aqueous environments, especially at an elevated temperature [3.1]. Therefore, subjecting adhesive joints to dynamic fatigue loads, whilst being immersed in water, is potentially a very demanding test environment, but one which is frequently encountered in a bonded structure.

However, apart from representing a real-life environment, it is also possible that the use of dynamic loading will accelerate the kinetics of the attack upon the joint by the ingressing water. Such an effect would be of some importance. Since other methods of accelerating the attack by water upon joints often involve greatly increasing the temperature, or applying unrealistically high static loads. These methods may drastically change the basic mechanism of joint failure, rather than merely accelerate the mechanism which is observed to occur during the service-life of the bonded structure.

As with other materials, the fatigue behaviour of adhesives and adhesive joints has been successfully studied employing a continuum fracture mechanics approach [3.1-3.9]. The early work by Mostovoy and Ripling [3.2] clearly established the validity of using a linear-elastic fracture-mechanics (LEFM) approach for describing the fatigue crack growth behaviour when bonding aluminium-alloy substrates using a range of epoxy-based adhesives. They employed a tapered-double cantilever-beam (TDCB) joint specimen, see Figure 3.1, and conducted the tests under nominally mode I (tensile-opening) cyclic loading and measured the rate of crack growth per cycle, da/dN, as a function of the applied range of strain-energy release-rate, ΔG, that was imposed. Where:

$$\Delta G = G_{max} - G_{min} \tag{3.1}$$

and here G_{max} is the maximum and G_{min} is the minimum value of the strain-energy release-rate applied per cycle. Firstly, they observed that, as for many other materials, over much of the range of experimental data the crack growth rate may be expressed by:

$$\frac{da}{dN} = A_f \Delta G^q \tag{3.2}$$

where A_f and q are constants. Secondly, their studies revealed that the relationship between da/dN and ΔG was actually sigmoidal in shape. Crack growth rates were found to decrease to very low values as ΔG approached some limiting threshold value, ΔG_{th}, and to increase to very high values as ΔG approached the typical value of the adhesive fracture energy, G_c, for crack growth under short-term monotonic loading conditions.

Subsequent work has, for example, studied the effects of the test frequency [3.2], thickness of the adhesive layer [3.7], the type of adhesive employed [3.3,3.4], the possibility of crack closure [3.3] and the mode-mix [3.5-3.6] of the loading conditions. (The 'mode-mix' being the ratio of mode I (tensile) to mode II (in-plane shear) loading.) More recently work [3.9] has also been undertaken on using the results from such fracture mechanics studies to predict the fatigue lifetime of adhesively-bonded joints.

The aim of the present work was to study the dynamic fatigue behaviour of joints which consisted of aluminium-alloy substrates bonded using an epoxy-based structural adhesive. One area of particular interest was the effect of conducting the fatigue tests in water, as well as in a relatively dry environment. A second theme of the work was to examine the effects of employing different surface pretreatments for the aluminium-alloy substrate, and to determine how the various pretreatments affect the resulting durability of the joint.

3.2 Experimental

3.2.1 The materials

The adhesive employed was a hot-curing toughened-epoxy, in the form of a film supported on a non-woven carrier. The adhesive was 'AF-163-2M' (from 3M Co., USA), with nominal thickness of 240 μm. The substrate was an aluminium alloy (Grade: British Standard 5083). This alloy contained 4.0 to 4.9 % magnesium and 1.0% manganese.

3.2.2 Joint preparation

The aluminium-alloy plate was either 11.0 mm or 12.7 mm in width (i.e. 'b' in Figure 3.1) and was machined, using a computer-controlled milling machine, into the tapered-cantilever beams shown in Figure 3.1. (These values of width, b, were more than sufficient to meet the ASTM [3.10] requirement for plane-strain conditions.) Before bonding, the substrates were either subjected to a chromic-acid etch [3.11] or a phosphoric-acid anodising [3.12] surface pretreatment. Also, in some instances, after phosphoric-acid anodising, a primer was applied to the surface. The primer was a corrosion-inhibiting primer, designated 'EC-3924B' and supplied by the 3M Co., USA. The primer was sprayed onto the surface of the aluminium alloy to give a thickness between about 1.25 to 3.5 μm and was dried by leaving the primed substrate at room temperature for 30 minutes and then placing it in an oven at 120^{o}C for about one hour.

Two pretreated aluminium-alloy beams were then bonded together to form a tapered-double cantilever-beam (TDCB) joint, see Figure 3.1. A 90 mm length of release-coated aluminium foil was placed at the narrow end of the TDCB joint to act as a starter crack. (This resulted in an initial (interfacial) crack length of about 75 mm.) The adhesive was then cured by heating the joint to 95^{o}C (as measured by a thermocouple placed in the adhesive layer) for 90 minutes and then raising the temperature to 120^{o}C for 30 minutes. The heat was then switched off and the joints were allowed to cool in the oven overnight. Whilst curing the adhesive joints were kept under a relatively low applied load. The glass transition temperature of the cured adhesive was 108^{o}C.

3.2.3 Determination of the adhesive fracture energy, G_c

Tests were conducted at a constant rate of displacement of the crosshead of the tensile testing machine in order to ascertain the value of the adhesive fracture energy, G_c, of the adhesive. The rate of displacement used for these monotonically-loaded tests was 1.0 mm/min.

LEFM is applicable to the bonded aluminium-alloy joints and the value of the adhesive fracture energy, G_c, may be calculated via the equation:

$$G_c = \frac{P_c^2}{2b} \cdot \frac{dC}{da} \qquad (3.3)$$

where P_c is the fracture load, b is the width of the specimen, C is the compliance ($C = \delta/P$; where δ is the displacement) and a is the crack length. For thin adhesive layers it has been shown [3.13] from beam theory that:

$$\frac{dC}{da} = \frac{8}{E_s b}\left(\frac{3a^2}{d^3} + \frac{1}{d}\right) \qquad (3.4)$$

where E_s is the modulus of the substrate arms, b is the width of the arms of the specimen and d is the height of the beam at a crack length a. Hence, combining Equations (3.3) and (3.4):

$$G_c = \frac{4P_c^2}{E_s b^2}\left(\frac{3a^2}{d^3} + \frac{1}{d}\right) \qquad (3.5)$$

Thus, the value of G_c may be deduced from the measured compliance of the specimen, via Equation (3.3). Alternatively, assuming the value of dC/da may be described using beam-theory, the value of G_c may be deduced via Equation (3.5).

3.2.4 Fracture mechanics data from the fatigue tests

The TDCB test specimen was used to obtain the values of da/dN as a function of the maximum strain-energy release-rate, G_{max}, applied in the fatigue cycle. A sine-wave loading-form was employed at a frequency of 5 Hz. A range of maximum displacements, δ_{max}, were employed in order to cover the complete range of applied fracture energy, G_{max}, values; i.e. the range from $G_{max} \cong G_{th}$ up to $G_{max} \cong G_c$. The displacement ratio ($\delta_{ratio} = \delta_{min}/\delta_{max}$) was 0.5. Displacement, rather than load, control was selected for the fatigue tests since it was found to be easier to detect the lower limit (i.e. the threshold value, G_{th}) of G_{max} using the former method of control. This is because with displacement control the value of G_{max} will decrease as the crack propagates through the TDCB specimen, and the crack growth rate, da/dN, will therefore decrease until it ceases altogether at the value of G_{th}.

It should be noted that G_{max} has been employed, as opposed to ΔG, since during the unloading part of the fatigue cycle the debonded surfaces typically come into contact, resulting in facial interference of the adhesive with itself (if cohesive-in-the-adhesive failure occurs) or with the metal surface (if interfacial failure occurs). This leads to the generation of surface debris which prevents the crack from fully closing when it is unloaded, and hence may give an artificially high value of G_{min}. Thus, it has been suggested [3.14,3.15] that it is better to use G_{max}, instead of ΔG; and this convention has been followed in the present studies. However, the choice of this approach does not significantly effect the general form of the fatigue crack-growth relationships.

For the tests conducted in the 'dry' environment, the test temperature was $23\pm1^{o}C$ and the relative humidity was 55%. For the tests conducted in the 'wet'

environment, the test temperature was 26±2°C and the joints were immersed in distilled water for about five minutes before the fatigue tests were started.

The crack length as a function of the number of cycles was determined either (i) by using a travelling microscope, with the side of the TDCB specimen painted white in order that the crack could be seen more clearly, or (ii) by using an automatic data acquisition system [3.16,3.17]. This system consisted of using an electrical potential method for measuring the length of the crack. The electrical potential method is an indirect d.c. potential technique and involved the use of a gauge bonded onto the side of the specimen, over the adhesive layer and adjacent substrates. The gauge was a plastic foil with a deposited metal film on its surface. The plastic foil provided both support and insulation from the metallic substrates. A small current of the order of 100 mA was passed through the foil, and when the crack propagated and broke the foil there was a large change in the resistance of the gauge, hence yielding a change in the d.c. potential. The change in potential was relayed from the leads soldered onto the gauge to an amplifier which gave a voltage reading. The signal was then relayed to a 'Mac Lab' data acquisition unit. The 'Mac Lab' was connected to a 'Macintosh PC'. The PC acquired the change in crack length as a function of the time (i.e. number of cycles) and a computer program, based on the ASTM Method E647-88 (see below), calculated the rate of crack growth per cycle, da/dN. The PC also acquired the signals of the maximum load and displacement being applied to the specimen, and therefore the corresponding value of G_{max} was deduced.

The maximum value of the strain-energy release-rate, G_{max}, applied during a fatigue cycle may be deduced using:

$$G_{max} = \frac{P_{max}^2}{2b}\frac{dC}{da} \qquad (3.6)$$

where P_{max} is the maximum load applied during the fatigue cycle. Alternatively, assuming the value of dC/da may be described using beam-theory, see Equation (3.4), the value of G_{max} may be deduced via Equation (3.7):

$$G_{max} = \frac{4P_{max}^2}{E_s b^2}\left(\frac{3a^2}{d^3} + \frac{1}{d}\right) \qquad (3.7)$$

If the fatigue data are plotted in the form of G_{max} versus da/dN, using logarithmic axes for both parameters, then a major portion of the relationship so obtained is often linear, as commented previously, and this region may be described by a form of the Paris Equation, namely:

$$\frac{da}{dN} = DG_{max}^n \qquad (3.8)$$

where D and n are material constants. Alternatively, the complete relationship between logarithmic G_{max} versus logarithmic da/dN is often of a sigmoidal form, which may be described by [3.9,3.14,3.15]:

$$\frac{da}{dN} = DG_{max}^{n}\left\{\frac{1-\left(\frac{G_{th}}{G_{max}}\right)^{n_1}}{1-\left(\frac{G_{max}}{G_c}\right)^{n_2}}\right\} \qquad (3.9)$$

where G_{th} is the minimum, or threshold, value of the applied strain-energy release-rate below which no fatigue crack growth is observed to occur, G_c is the value of the adhesive fracture energy from the constant rate of displacement tests and D, n, n_1 and n_2 are material constants.

The method employed for obtaining values of the crack growth rate per cycle, da/dN, was that described as the 'incremental polynomial method' in ASTM E647-88 [3.18]. Several methods have been investigated [3.15] for deducing the value of da/dN associated with a given crack length from the experimental measurements of crack length, a, versus number of cycles, N. The 'incremental polynomial method' was found to be the most accurate, and the one that gave the lowest scatter.

3.3 Results and Discussion

3.3.1 Compliance of the TDCB joint

To validate the experimental techniques, the compliance of the TDCB joint was deduced by plotting the compliance, C, versus the crack length, a; where the crack length was determined (i) visually, using a travelling microscope, and (ii) employing the automatic monitoring system. The resulting slopes, dC/da, of the linear plots so obtained are shown in Table 3.1. As may be seen, the agreement between the experimental methods is excellent. Further, the agreement between the experimental values and the theoretically calculated value, using Equation (3.4), is also excellent.

Table 3.1 Compliance calibration results

Method	$dC/da\ (x\ 10^{-5})\ (N^{-1})$
Experimental - visual	$2.10 \pm 12\%$
Experimental - automatic	$2.05 \pm 6\%$
Theoretical (Equation 3.4)	2.10

Notes:

(i) $b = 11.0$ mm;

(ii) The coefficients of variation are given for the experimental measurements.

However, it should be noted that the above results were obtained under the 'dry' test conditions, either at a constant rate of displacement or under cyclic fatigue loading. When similar studies were conducted under the 'wet' cyclic fatigue conditions, then it was found that the experimentally determined value of the compliance of the joint was often significantly higher than the theoretical value. This was considered to be due to water uptake and plasticisation of the adhesive, particularly in the highly-stressed regions ahead of the crack. These effects would obviously soften the adhesive and could lead to an increase in the compliance of the TDCB joint. Therefore, for the fatigue tests undertaken in the 'wet' test conditions, Equation (3.6) was used to deduce the value of G_{max}, using the experimentally deduced value of dC/da.

3.3.2 G_c of the adhesive

For the fracture tests conducted at a constant rate of displacement of 1 mm/min the crack always propagated cohesively through the adhesive layer in a stable manner; i.e. the interfacial initial ('starter') crack did not continue to propagate along the interface, but instead diverted into the adhesive layer to give a cohesive fracture. Therefore, as would be expected, there was no dependence of the value of the adhesive fracture energy, G_c, upon the type of surface pretreatment employed for the aluminium-alloy substrates prior to bonding.

Further, there was no dependence of the value of G_c upon the length of the propagating crack; so no 'resistance-curve' (i.e. 'R-curve') was observed for this adhesive. The values of G_c determined from either Equations (3.3) or (3.5) were in excellent agreement, as revealed by the results discussed above. The measured value of G_c was 1720 J/m^2.

3.3.3 Fatigue data from the TDCB joints - 'dry' environment

As was observed for the constant rate of displacement tests, during the fatigue tests in the 'dry' environment (i.e. at a test temperature of 23±1°C and a relative humidity of 55%) the crack propagated cohesively through the adhesive layer in a stable manner. Thus, there was no significant dependence of the fatigue behaviour upon the surface pretreatment which had been employed for the substrates.

A typical graph of da/dN versus G_{max}, where the value of G_{max} was determined using Equation (3.6), is shown in Figure 3.2; using logarithmic scales. The fatigue data, taken together with the value of G_c, reveal a curve which is sigmoidal in shape with three clearly distinguishable regions:

(i) 'Region I' which is a threshold region, and which is associated with very low values of da/dN and G_{max},

(ii) 'Region II' which is the linear portion.

(iii) 'Region III' where the value of G_{max} starts to approach that of G_c.

In 'region I' the presence of a threshold, below which no significant fatigue crack growth occurs, is clearly visible. Indeed, the data in this 'region I' part of the curve show that the values for fatigue crack growth rate, da/dN, are about 10^{-7} mm/cycle, and this meets the ASTM [3.18] requirement for the value of da/dN to be considered to be negligible. The value of G_{th} is about 560 J/m^2. It should be noted that this value of G_{th} is far lower than the adhesive fracture energy, G_c, measured under the monotonic-loading test conditions. Indeed, the value of the threshold value, below which fatigue crack growth is not observed, is approximately 30% of the static value.

3.3.4 Fatigue data from the TDCB joints - 'wet' environment

3.3.4.1 Introduction

Cyclic fatigue tests were also conducted in the 'wet' environment, namely in water at 26±2°C. Again crack growth always occurred in a stable manner. The results are shown in Figure 3.3, where the fatigue results from the 'dry' tests are also plotted. Several interesting points may be noted from these results.

3.3.4.2 Chromic-acid etched (CAE) pretreated joints

For the chromic-acid etched (CAE) pretreated joints, firstly, when relatively low values of the maximum displacement (i.e. δ_{max} values of 1.4 and 1.6 mm) were used, then an interfacial locus of joint failure was visually observed and the fatigue behaviour of the 'wet' tests was greatly inferior to that shown by the 'dry' tests. Thus, in these joints, the water attacked and weakened the interfacial

regions. This is reflected in the value of G_{th} being about 45 J/m^2. It should be recalled from the previous discussions that the value of G_c was 1720 J/m^2. Hence, the 'wet' value of G_{th} for the CAE pretreated joints was only about 3% of the value of the adhesive fracture energy, G_c.

However, secondly, the results for the fatigue experiments conducted at a relatively high maximum displacement (i.e. at δ_{max} values of 2.6 mm) revealed that the locus of failure was again via cohesive fracture through the adhesive layer, as observed for the 'dry' tests, see above. However, these fatigue results for the 'wet - δ_{max}=2.6 mm' tests (shown by the 'o' points in Figure 3.3) do show a somewhat inferior fatigue behaviour to those from the previous 'dry' tests. Now, the fact that the locus of failure remained cohesive is suggested to arise from the high maximum displacement used in these fatigue tests. This caused the test to be finished in a very short timescale, before the water could attack the interface. Indeed, the time involved for complete joint failure was only a few hours. The inferior fatigue resistance of these joints tested in the 'wet' environment, where δ_{max} values of 2.6 mm were used, compared to those tested in the 'dry' environment is suggested to be due to plasticisation of the adhesive at the crack tip by the ingressing water. This could well weaken the adhesive directly ahead of the crack tip and so allow somewhat faster fatigue crack growth to occur.

3.3.4.3 Phosphoric-acid anodised (PAA) pretreated joints

In the case of the PAA treated joints, then these joints were prepared using either (i) a PAA pretreatment, or (ii) a PAA pretreatment followed by application of the 'EC-3924B' primer, for the aluminium-alloy substrate. Firstly, it was found that upon conducting the experiments in water at 26^{o}C that, at all values of the applied maximum displacement, δ_{max}, the locus of failure remained cohesive in the adhesive layer, as indicated in Figure 3.3. Hence, no major decreases in the fatigue behaviour for the PAA, or PAA and primed, joints were ever observed; even when the test lasted longer than ten days or so, with the value of G_{max} then being equal to G_{th}. This should be contrasted to the results recorded for the CAE treated joints. Here, apart from the fatigue tests of very short duration (i.e. at δ_{max} values of 2.6 mm), water attack upon the interfacial regions of the CAE pretreated joints led to interfacial failure occurring, which was accompanied by a dramatic reduction in the fatigue resistance, as described above.

Secondly, there was however a relatively small decrease in the fatigue resistance of the PAA, and PAA and primed, joints when they tested in the 'wet' environment. This small decrease was of the same order as observed for the CAE pretreated joints when the relatively high value of maximum displacement (i.e. a δ_{max} value of 2.6 mm) was employed, and cohesive failure was also recorded in these joints. In the case of the PAA pretreated joints the slight decrease in fatigue resistance when tested in the 'wet' environment is again presumably due to plasticisation of the adhesive ahead of the crack tip by ingressing water.

Thirdly, again a well-defined threshold value was apparent, and the value of G_{th} was about 310 J/m^2. This represents approximately 20% of the initial (monotonically-loaded) value of G_c which was obtained, the value of G_c being 1720 J/m^2. The above observations apply equally to whether the treatment used was either (i) a PAA pretreatment, or (ii) a PAA pretreatment followed by the 'EC-3924B' primer.

3.3.5 Comparison of data

The above results are brought together in Table 3.2, which shows the values of the adhesive fracture energy, G_c, the threshold strain-energy release rate, G_{th}, obtained from the cyclic fatigue tests and the locus of joint failure. They clearly reveal several interesting observations.

Firstly, under constant rate of displacement (i.e. monotonic-loading) and 'dry' fatigue test conditions all the different surface pretreatments give a locus of joint failure which is cohesive through the adhesive layer.

Secondly, however, the fatigue tests clearly reveal the damaging effect of cyclic-loading conditions compared to simply employing a constant rate of displacement to fracture the adhesive joint. Indeed, the value of the threshold strain-energy release-rate, G_{th}, is far lower than the value of the adhesive fracture energy, G_c, which is obtained under monotonic loading.

Thirdly, under the 'wet' fatigue test conditions the effects of water on the CAE treated joints is dramatic, with the locus of failure changing from cohesive to interfacial, between the adhesive and aluminium-alloy substrate; and the value of G_{th} being greatly decreased.

Fourthly, however, this deleterious attack by moisture is not seen if the substrates are pretreated prior to joint manufacture using either the phosphoric-acid anodising treatment, or the phosphoric-acid anodising treatment followed by application of the primer. In these joints the locus of failure was still cohesive through the adhesive layer, although there was a small decrease in the value of G_{th} from the 'wet' tests, compared to the value of G_{th} obtained from the 'dry' tests. This was considered to arise from water plasticising the adhesive directly ahead of the crack tip, and so weakening the material and allowing somewhat more rapid and easier fatigue crack growth to occur.

Finally, it should noted that the fatigue tests at the relatively low maximum displacements (i.e. applied δ_{max} values of 1.4 and 1.6 mm) in the 'wet' environment typically lasted about two to three weeks. Thus, the fatigue data determined from towards the end of the test were associated with regions of the TDCB joint which had been exposed longer to the aqueous environment than regions from which the earlier test data had been obtained. Other work [3.16] has been concerned with the possible interactions between the rate of fatigue crack growth along a TDCB specimen and water diffusion (and attack on the interfacial regions of the joint) ahead of the advancing fatigue crack. However, work on a

similar adhesive system has shown that exposing the TDCB joint to the aqueous environment, but in an unstressed condition, for up to about one year had no significant effect on the subsequent fatigue curve which was determined in the 'wet' environment.

Table 3.2 Comparison of main results

Surface pretreatment	Monotonic tests		Fatigue tests	
	G_c (J/m^2)	LoF	G_{th} (J/m^2)	LoF
'Dry' environment:				
CAE	1720	Coh.	560	Coh.
PAA	1720	Coh.	560	Coh.
PAA + primer	1720	Coh.	560	Coh.
'Wet' environment:				
CAE	-	-	45	Interf.
PAA	-	-	310	Coh.
PAA + primer	-	-	310	Coh.

Notes:

a. LoF: locus of joint failure.
Coh.: cohesive in the adhesive layer.
Interf.: visually interfacial between the adhesive and aluminium-alloy substrate.

3.4 Conclusions

A fracture mechanics approach has been successfully used to examine the cyclic fatigue behaviour of bonded joints, which consisted of aluminium-alloy substrates bonded using a toughened-epoxy structural adhesive. As previously reported, cyclic fatigue tests conducted in a relatively dry environment of 23^{o}C and 55% r.h. lead to joint failure at far lower loads, and far lower values of the maximum strain-energy release-rate, G_{max}, applied in a fatigue cycle compared to the value of the adhesive fracture energy, G_c, determined from monotonically-loaded fracture tests. For example, the value of G_{th} from the 'dry' fatigue tests was about 560 J/m^2, whilst the value of the adhesive fracture energy, G_c, was 1720 J/m^2.

Cyclic fatigue tests were also conducted in a 'wet' environment, namely immersion in water at 26°C. These 'wet' fatigue tests clearly revealed the dramatic effect an aggressive, hostile environment may have upon the mechanical performance of an adhesive joint.

However, the fatigue tests demonstrated that a threshold value of the applied strain-energy release-rate, G_{th}, does exist and may be used to rank the fatigue limit behaviour of different adhesive systems and their resistance to hostile environments. For example, for the joints where the aluminium-alloy substrates were chromic-acid etched prior to bonding, the value of G_{th} from the 'wet' fatigue tests was about 45 J/m^2, and the locus of joint failure was visually assessed to be interfacial between the adhesive and aluminium-alloy. Hence, this value of G_{th} from the 'wet' fatigue tests on the CAE pretreated joints was only about 3% of value of the adhesive fracture energy, G_c. On the other hand, the 'wet' fatigue tests clearly revealed that the use of either (i) a phosphoric-acid anodised (PAA) pretreatment, or (ii) a PAA pretreatment followed by the application of a primer, for the aluminium-alloy substrates leads to the locus of joint failure remaining cohesive through the adhesive layer. Further, for these PAA, or PAA and primed, pretreated joints, the value of G_{th} was only slightly decreased compared to the value obtained from the 'dry' fatigue tests. Therefore, such pretreatments for the aluminium-alloy substrates imparted excellent durability to the adhesively-bonded joints.

Now, a major advantage of the 'wet' cyclic fatigue tests is that they may be undertaken and completed in the matter of a few weeks and do not require the use of unrealistically high temperatures or applied (static) loads in order to accelerate the mechanism of water attack upon the joints. The use of unrealistically high temperatures or applied (static) loads may actually lead to the joints weakening due to <u>new</u> mechanisms of attack, as opposed to merely accelerating the same mechanisms as seen in the normal service environment which the joint experiences. Thus, the development and standardisation of 'wet' cyclic fatigue tests may provide the basis for a very effective accelerated-ageing test.

The presence of a threshold value of the applied strain-energy release rate, G_{th}, below which no fatigue failure occurs, also has important implications for the design of adhesive joints. Obviously, if the applied loads on the joint are kept below a level corresponding to the value of G_{th}, then joint failure should not be observed, making due allowance of course for suitable safety factors. However, it is of importance to investigate whether simply ageing the joints in water (i.e. immersing them, under no load, in water) for a relatively long period before undertaking the 'wet' fatigue tests would significantly affect the value of G_{th}.

3.5 References

3.1.	A.J. Kinloch,	'Adhesion and Adhesives: Science and Technology' (Chapman and Hall, London, 1983) p 339
3.2.	S. Mostovoy and E.J.Ripling,	in 'Adhesion Science and Technology' L.H. Lee, (Ed.) (Plenum Press, New York, 1975), p 514
3.3.	D.A. Jablonski,	'Fatigue crack growth in structural adhesives' J. Adhesion **11** (1980) p 125
3.4.	S. Mall and K.T. Yun,	'Effect of adhesive ductility on cyclic debond mechanism' J. Adhesion **23** (1987) p 215
3.5.	C. Lin and K.M. Liechti,	'Similarity concepts in the fatigue fracture of adhesively bonded joints' J. Adhesion **21** (1987) p 1
3.6.	S. Mall and W.S. Johnson,	'Debonding characteristics of adhesively bonded woven Kevlar composites', ASTM STP **981** (1988) p 194
3.7.	S. Mall and G. Ramamurthy,	'Effect of bond thickness on fracture and fatigue strength of adhesively bonded composite joints' Int. J. Adhesion Adhesives **9** (1989) p 33
3.8.	D.W. Schumeser,	'A fracture mechanics approach to characterising cyclic debonding' J. Adhesion, **36** (1991) p 1
3.9.	A.J. Kinloch and S.O. Osiyemi,	'Predicting the fatigue life of adhesively-bonded joints' J. Adhesion **43** (1993) p 79
3.10.	ASTM,	'Standard test method for plane-strain fracture toughness and strain-energy release rate of plastic materials' D 5045 (1991)
3.11.	Ministry of Defence,	'Defence specification', UK 03-2/1 (1970)
3.12.	Boeing Aeroplane Company,	'Surface Treatment Specification', Boeing, USA, BAC 5555
3.13.	A.J. Kinloch,	'Adhesion and Adhesives: Science and Technology' (Chapman and Hall, London, 1983) p 264

3.14. R.H. Martin and G.B. Murri, 'Characterisation of mode I and mode II delamination growth and thresholds in AS4/PEEK composites' ASTM STP **1059** (1990) p 251

3.15. S.O. Osiyemi, 'The fatigue performance of adhesively bonded fibre-composite joints', (Ph.D Thesis, Univ. of London, 1992), p 83

3.16. J.K. Jethwa, 'The fatigue performance of adhesively-bonded metal joints', (Ph.D Thesis, Univ. of London, 1995)

3.17. J.K. Jethwa and A.J. Kinloch, 'The fatigue performance of adhesively-bonded metal joints', Proc. 17th Annual Meeting of the US Adhesion Soc., Florida, USA, February, 1994

3.18. ASTM, 'Standard test method for measurement of fatigue crack growth rates' E647 (1988)

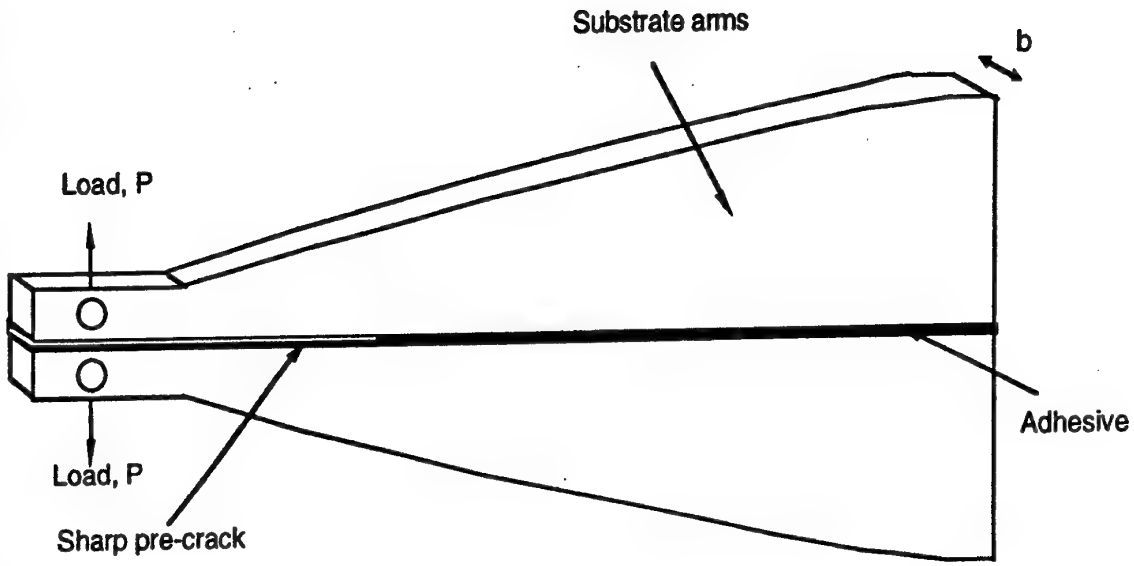

Figure 3.1 A sketch of the tapered-double cantilever-beam (TDCB) adhesively-bonded joint.

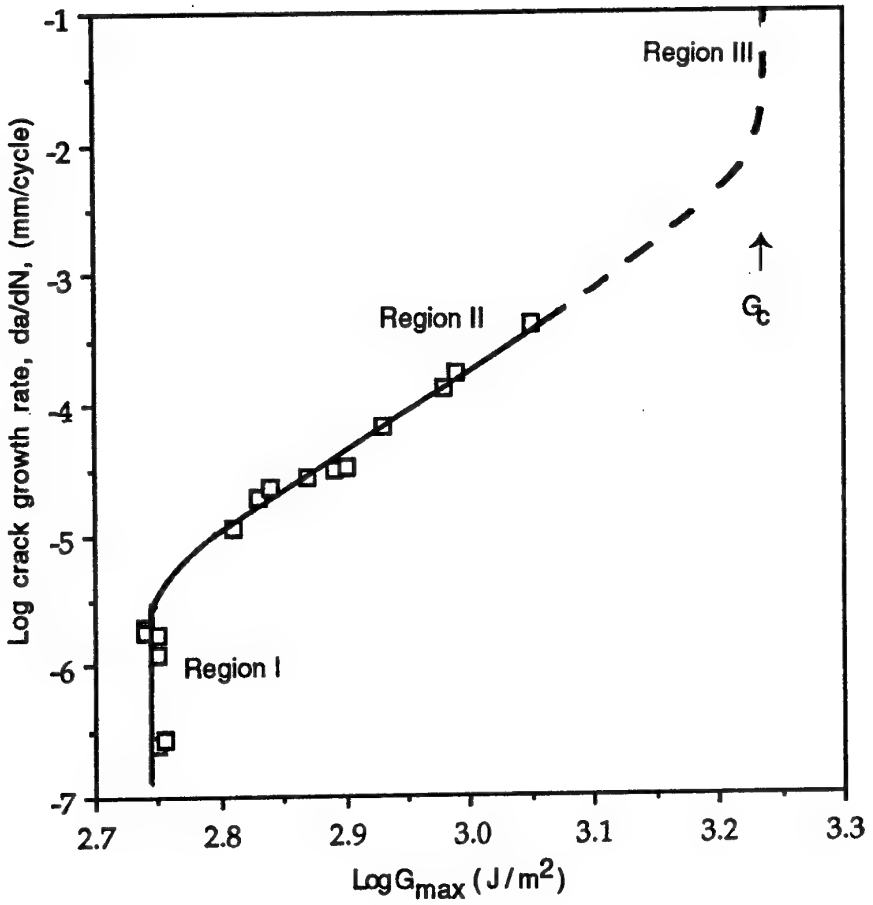

Figure 3.2 Logarithmic crack growth rate per cycle, da/dN, versus logarithmic G_{max} for the joints prepared using the CAE pretreatment for the aluminium-alloy substrates and bonded using the epoxy-film adhesive.The fatigue tests were conducted in the 'dry' environment of 23^{o}C and 55% r.h. (TDCB joint tests.)

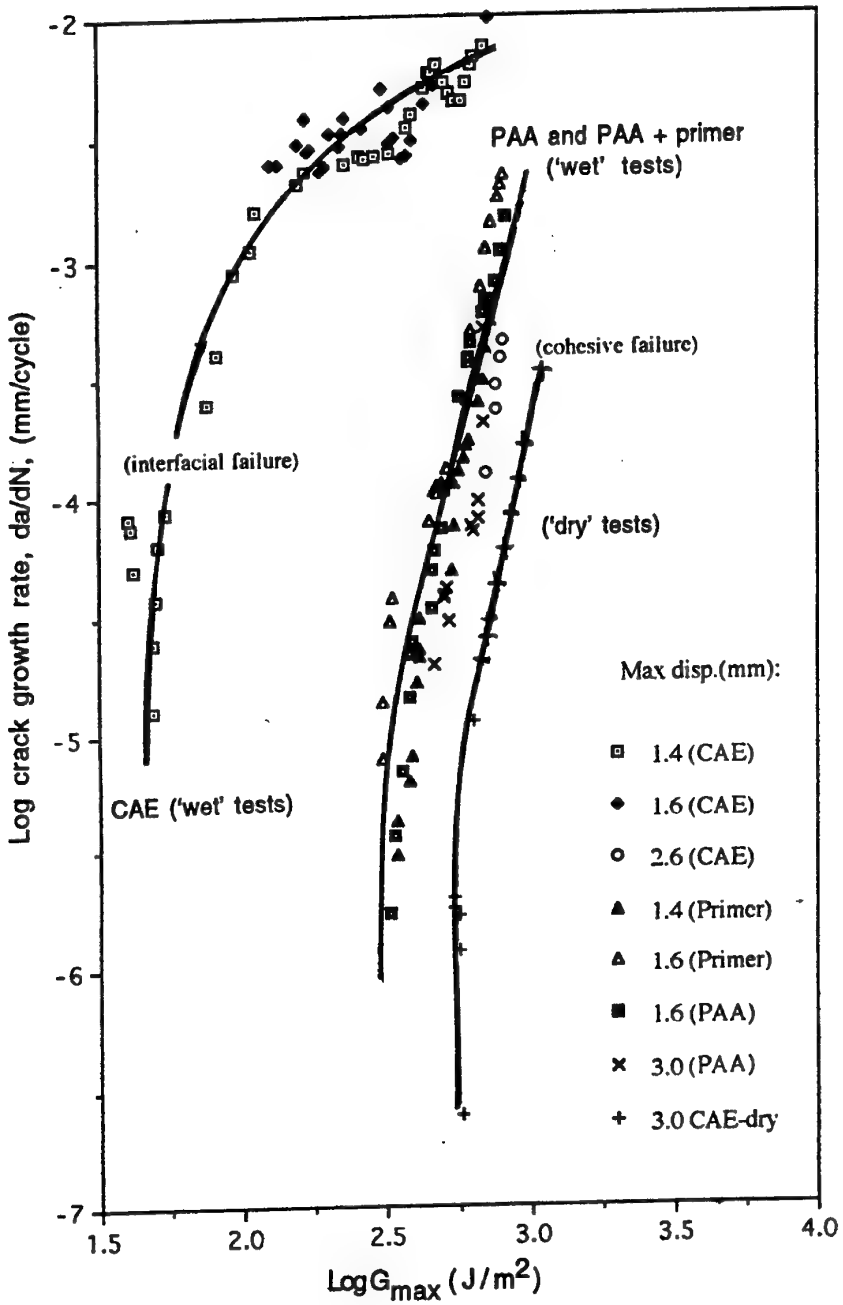

Figure 3.3 Logarithmic crack growth rate per cycle, da/dN, versus logarithmic G_{max} for all the different types of joints tested in both the 'dry' and 'wet' environments. The main type of joint and test environment associated with a given set of data are stated. (TDCB joint tests.)

[Also given is the maximum displacement, δ_{max}, for each test - the tests were undertaken in the 'wet' environment, unless otherwise stated.]

SECTION 4

CONCLUDING REMARKS

4.1. Introduction

The current programme has focussed on the adhesive bonding of fibre-composites, based upon thermoplastic polymeric matrices, and the bonding of aluminium alloys. In both cases a structural epoxy-film adhesive has been employed.

4.2 Main Conclusions

4.2.1 The adhesively-bonded fibre-composite joints

4.2.1.1 The bonded carbon-fibre/PEEK joints

1. For the carbon-fibre/PEEK joints it was found that a simple abrasion/solvent wipe pretreatment gave very, very low joint strengths, with failure occurring at the adhesive/composite interface. Therefore, an additional corona or plasma treatment stage is needed for the thermoplastic composite prior to bonding. The level of corona treatment needed to obtain cohesive failure through the adhesive for the carbon-fibre/PEEK was about 30 J/mm^2. Both corona and plasma treatments of the carbon-fibre/PEEK composite prior to bonding were found to be adequate to avoid interfacial failure, and the associated weak joints. For the carbon-fibre/PEEK joints which were so-treated, the value of the adhesive fracture energy, G_c, was 1300 J/m^2. The locus of joint failure was via a cohesive failure through the adhesive layer.

2. As was observed for the constant rate of displacement tests, for the corona treated carbon-fibre/PEEK substrates bonded using the epoxy film-adhesive, during the fatigue tests the crack propagated cohesively through the adhesive layer in a stable manner. A typical graph of logarithmic da/dN versus logarithmic G_{max}, where the value of G_{max} is the maximum strain-energy release rate applied in a cycle, showed that the agreement between the duplicate tests for the fatigue experiments conducted in the 'dry' environment of 23±1°C and 55% r.h. was very good.

3. There was no significant effect of undertaking the fatigue tests in the 'wet' environment, where the test temperature was 26±2°C and the joints were immersed in distilled water for about five minutes before the fatigue tests were started.

4. The fatigue data may be described by a power-law relationship.

5. For the studies on the single-overlap joints loaded in tension, the carbon-fibre/PEEK substrates were again subjected to a level of corona treatment of about 30 J/mm^2 prior to being bonded. This gave a cohesive failure through the adhesive with a static lap joint strength of 41 MPa.

6. The fatigue behaviour of the lap joints was also measured. The relationship between the maximum load per unit width, T_{max}, and the number of cycles to failure, N_f, could be predicted extremely well from the fracture mechanics data.

4.2.1.2 The bonded glass-fibre/PPS joints

1. For the glass-fibre/PPS substrates bonded also using the epoxy-film adhesive, the first set of tests used a simple abrasion and solvent wipe treatment for the prior to bonding. The DCB joints were then prepared and tested and it was found that all the joints failed by interlaminar failure of the fibre-composite.

2. Now it was thought that some form of corona or plasma treatment for the fibre-composite substrates would have been necessary in order to prevent interfacial failure occurring at the composite/adhesive interface. Clearly this was not the case. The reasons for the observation that just a simple abrasion/solvent wipe treatment appears to be adequate to avoid interfacial failure were considered to be:

(i) The presence, and exposure by the surface treatment of the glass fibres - glass has a high surface energy and is therefore a relatively easy material to bond.

(ii) The low transverse strength of the glass-fibre/PPS composite, compared to the high transverse tensile-stresses generated around the inserted interfacial crack. (Indeed, the transverse strength of the glass-fibre/PPS composite was measured and found to be about 8.6±0.2 MPa, which is extremely low.)

(iii) The above factors lead to the fact that interlaminar failure is seen at a relatively low load, before interfacial failure can occur.

3. However, the above factors are reflected in the fact that the value of the adhesive fracture energy, G_c, for the onset of crack growth is about 600±100 J/m^2. This is far lower than the value of 1300 J/m^2 recorded for the carbon-fibre/PEEK joints when the locus of failure was cohesive in the adhesive.

4. To try and study the above effects in a practical design of joint, the glass-fibre/PPS composite was bonded to form a single overlap joint. Again, a simple abrasion and solvent wipe treatment was used for the glass-fibre/PPS substrates prior to bonding. The lap joints were then prepared and a series of joints were made with a varying adhesively-bonded overlap length. They were tested at a constant rate of displacement and it was found that all the joints failed by interlaminar failure of the fibre-composite, even when a relatively long overlap length was employed.

4.2.2 The adhesively-bonded aluminium-alloy joints

1. A fracture mechanics approach has been successfully used to examine the cyclic fatigue behaviour of bonded joints, which consisted of aluminium-alloy substrates bonded using a toughened-epoxy structural adhesive. As previously reported, cyclic fatigue tests conducted in a relatively dry environment of 23°C and 55% r.h. lead to joint failure at far lower loads, and far lower values of the maximum strain-energy release-rate, G_{max}, applied in a fatigue cycle compared to the value of the adhesive fracture energy, G_c, determined from monotonically-loaded fracture tests. For example, the value of G_{th} from the 'dry' fatigue tests was about 560 J/m^2, whilst the value of the adhesive fracture energy, G_c, was 1720 J/m^2.

2. Cyclic fatigue tests were also conducted in a 'wet' environment, namely immersion in water at 26°C. These 'wet' fatigue tests clearly revealed the dramatic effect an aggressive, hostile environment may have upon the mechanical performance of an adhesive joint.

3. However, the fatigue tests demonstrated that a threshold value of the applied strain-energy release-rate, G_{th}, does exist and may be used to rank the fatigue limit behaviour of different adhesive systems and their resistance to hostile environments. For example, for the joints where the aluminium-alloy substrates were chromic-acid etched prior to bonding, the value of G_{th} from the 'wet' fatigue tests was about 45 J/m^2, and the locus of joint failure was visually assessed to be interfacial between the adhesive and aluminium-alloy. Hence, this value of G_{th} from the 'wet' fatigue tests on the CAE pretreated joints was only about 3% of value of the adhesive fracture energy, G_c. On the other hand, the 'wet' fatigue tests clearly revealed that the use of either (i) a phosphoric-acid anodised (PAA) pretreatment, or (ii) a PAA pretreatment followed by the application of a primer, for the aluminium-alloy substrates leads to the locus of joint failure remaining cohesive through the adhesive layer. Further, for these PAA, or PAA and primed, pretreated joints, the value of G_{th} was only slightly decreased compared to the value obtained from the 'dry' fatigue tests. Therefore, such pretreatments for the aluminium-alloy substrates imparted excellent durability to the adhesively-bonded joints.

4. Now, a major advantage of the 'wet' cyclic fatigue tests is that they may be undertaken and completed in the matter of a few weeks and do not require the use of unrealistically high temperatures or applied (static) loads in order to accelerate the mechanism of water attack upon the joints. The use of unrealistically high temperatures or applied (static) loads may actually lead to the joints weakening due to <u>new</u> mechanisms of attack, as opposed to merely accelerating the same mechanisms as seen in the normal service environment which the joint experiences. Thus, the development and standardisation of 'wet' cyclic fatigue tests may provide the basis for a very effective accelerated-ageing test.

5. The presence of a threshold value of the applied strain-energy release rate, G_{th}, below which no fatigue failure occurs, also has important implications for the design of adhesive joints. Obviously, if the applied loads on the joint are kept below a level corresponding to the value of G_{th}, then joint failure should not be observed, making due allowance of course for suitable safety factors. However, it is of importance to investigate whether simply ageing the joints in water (i.e. immersing them, under no load, in water) for a relatively long period before undertaking the 'wet' fatigue tests would significantly affect the value of G_{th}.

4.2.3 Comparisons between the types of bonded joints.

1. One obvious point of difference between the results from the bonded carbon-fibre/PEEK and aluminium-alloy joints is that the respective values of the adhesive fracture energy, G_c, are 1300 J/m^2 and 1720 J/m^2. In both cases the locus of failure is cohesive through the epoxy-film adhesive. This effect of the substrate on the measured value of G_c has been reported previously, and is considered to be due to the substrate affecting the stress-field, and hence the degree of plasticity, ahead of the crack.

2. The higher values of G_c for the aluminium-alloy joints is also seen in the superior fatigue behaviour of these joints compared to the carbon-fibre/PEEK joints.

3. On the other hand, the carbon-fibre/PEEK joints were not significantly affected by undertaking the fatigue tests in the 'wet', as opposed to the 'dry', environment. Whether, or not, the aluminium-alloy joints were significantly affected by undertaking the fatigue tests in the 'wet', as opposed to the 'dry', environment was dependent upon the type of surface treatment employed for the aluminium-alloy substrates prior to bonding.

4. The glass-fibre/PPS joints gave a relatively poor performance compared to the carbon-fibre/PEEK joints. This was due to the glass-fibre/PPS substrates delaminating under relatively low stresses. This effect also resulted in the glass-fibre/PPS substrates not requiring a relatively complex corona or plasma treatment prior to bonding.

5. However, if a glass-fibre/PPS material is developed with a substantially higher transverse tensile-strength it may be that a corona or plasma treatment would be required prior to bonding, in order to avoid premature interfacial failure and associated weak joints.

4.3 Suggestions for Future Work

1. Future work is needed to investigate the effect of exposing joints to the aqueous environment, in an **unstressed condition**, for relatively long periods of time, prior to then conducting fatigue tests in the 'wet' environment. The aim is to see whether the storage period significantly affects the fatigue behaviour. If not, then the fatigue tests conducted in a 'wet' environment will prove to be both excellent test methods for comparing different adhesive systems and for predicting accurately the long term fatigue life of various designs of bonded joints.

2. So far, only mode I (tensile opening) tests have been conducted. The other types of loadings (for example, mode II (in-plane shear) and mixed-mode I/II loadings) should be studied.

3. The predictive analysis outlined in the current report should be studied further. In particular, it should be applied to other types of joint designs, including some actual bonded components.

4. The predictive model described in the present report in an analytical model. It should be compared to a model based upon finite-element analysis methods, since such an approach is capable of greater flexibility when other joint designs are employed.

SECTION 5

ACKNOWLEDGEMENTS

The authors are pleased to acknowledge the support and sponsorship of this work by the U.S. Government through its European Research Office of the U.S. Army. They would also like to thank especially Drs. S. Wentworth and M. Sennett (US Army) for their support and encouragement during this programme.